
Doctoral Dissertations

Student Theses and Dissertations

1970

Temperature variation in distribution of relaxation times in aluminosilicate glasses

David Wayne Moore

Follow this and additional works at: https://scholarsmine.mst.edu/doctoral_dissertations



Part of the [Ceramic Materials Commons](#)

Department: **Materials Science and Engineering**

Recommended Citation

Moore, David Wayne, "Temperature variation in distribution of relaxation times in aluminosilicate glasses" (1970). *Doctoral Dissertations*. 2288.

https://scholarsmine.mst.edu/doctoral_dissertations/2288

This thesis is brought to you by Scholars' Mine, a service of the Missouri S&T Library and Learning Resources. This work is protected by U. S. Copyright Law. Unauthorized use including reproduction for redistribution requires the permission of the copyright holder. For more information, please contact scholarsmine@mst.edu.

TEMPERATURE VARIATION IN DISTRIBUTION OF RELAXATION
TIMES IN ALUMINOSILICATE GLASSES

by

DAVID WAYNE MOORE, 1938-⁴³⁵⁷³

A DISSERTATION

Presented to the Faculty of the Graduate School of the

UNIVERSITY OF MISSOURI - ROLLA

In Partial Fulfillment of the Requirements for the Degree

DOCTOR OF PHILOSOPHY

in

CERAMIC ENGINEERING

1970

T2359
82 pages
c.1

Delbert E. Day
Advisor

Robert E. Moore

J. Earl Foster

Peter J. Hansen

Robert L. Davis

187437

ABSTRACT

The distribution of relaxation times for the alkali peak in a $\text{Li}_2\text{O}\cdot\text{Al}_2\text{O}_3\cdot 2.0\text{SiO}_2$ glass and for the mixed alkali peak in a $0.5\text{Li}_2\text{O}\cdot 0.5\text{Na}_2\text{O}\cdot\text{Al}_2\text{O}_3\cdot 2.0\text{SiO}_2$ glass was studied using the internal friction technique. A lognormal distribution of relaxation times provided the best agreement with the experimental data. The β parameter of the lognormal distribution function, which is related to the half-height peak width, varied with temperature, indicating that the distribution of relaxation times is dependent upon the activation energy and the activation entropy of the relaxation mechanism. The major contributor to the distribution of relaxation times is a wide distribution in the activation entropy, while the distribution in activation energy is relatively narrow. No noticeable change in internal friction was found when precautions were taken to eliminate any surface water on a specimen.

ACKNOWLEDGEMENT

The author wishes to thank Dr. Delbert E. Day, major Ph.D. advisor, for his guidance and advice relating to this thesis, Mr. James C. Pool and Mr. Gary L. McVay, fellow graduate students, for their informal discussions concerning internal friction in glass, and the United States Government for financial support received through a N.D.E.A. Title IV fellowship.

Most sincerely the author expresses his gratitude and appreciation to his wife for putting up with many years in graduate school.

TABLE OF CONTENTS

	Page
ABSTRACT.....	ii
ACKNOWLEDGEMENT.....	iii
LIST OF ILLUSTRATIONS.....	v
LIST OF TABLES.....	vii
I. INTRODUCTION.....	1
II. EXPERIMENTAL PROCEDURE.....	6
A. Sample Preparation.....	6
B. Internal Friction Measurements.....	7
C. Activation Energy.....	8
III. RESULTS.....	10
IV. DISCUSSION.....	13
A. Relaxation Time Distribution Function.....	13
B. Long Tail of the Experimental Data.....	16
C. β Variation with Temperature.....	18
D. Distribution in Activation Energy and Activation Entropy.....	20
V. CONCLUSIONS.....	26
VI. APPENDICES.....	46
A. Chemical Analysis of Raw Materials.....	47
B. Peak Height Determination and Correction.....	50
C. Figures of Experimental Data.....	56
D. Derivation of Internal Friction Equation Based on Lognormal Distribution of Relaxation Times.....	69
VII. BIBLIOGRAPHY.....	71
VIII. VITA.....	75

LIST OF ILLUSTRATIONS

Figures	Page
1. Annealing Cycle, $\text{Li}_2\text{O}\cdot\text{Al}_2\text{O}_3\cdot 2.0\text{SiO}_2$ Glass.....	27
2. Annealing Cycle, $0.5\text{Li}_2\text{O}\cdot 0.5\text{Na}_2\text{O}\cdot\text{Al}_2\text{O}_3\cdot 2.0\text{SiO}_2$ Glass.....	27
3. Block Diagram of Sonic Damping Equipment.....	28
4. Schematic Diagram of Torsion Pendulum.....	29
5. Typical Internal Friction Curve, $\text{Li}_2\text{O}\cdot\text{Al}_2\text{O}_3\cdot 2.0\text{SiO}_2$ Glass, Frequency 0.76 HZ.....	30
6. Typical Internal Friction Curve, $0.5\text{Li}_2\text{O}\cdot 0.5\text{Na}_2\text{O}\cdot$ $\text{Al}_2\text{O}_3\cdot 2.0\text{SiO}_2$ Glass, Frequency 0.644 HZ.....	31
7. Comparison of Internal Friction Data on Torsion Pendulum and Sonic Damping Equipment, $\text{Li}_2\text{O}\cdot\text{Al}_2\text{O}_3\cdot$ 2.0SiO_2 Glass, Frequency (1) 0.0734 HZ., (2) 1.20 HZ. (3) 3293 HZ.....	32
8. Comparison of Internal Friction Data on Torsion Pendulum and Sonic Damping Equipment, $0.5\text{Li}_2\text{O}\cdot$ $0.5\text{Na}_2\text{O}\cdot\text{Al}_2\text{O}_3\cdot 2.0\text{SiO}_2$ Glass, Frequency (1) 0.0914 HZ., (2) 1.044 HZ., (3) 2751 HZ.....	33
9. Activation Energy, $\text{Li}_2\text{O}\cdot\text{Al}_2\text{O}_3\cdot 2.0\text{SiO}_2$ Glass.....	34
10. Activation Energy, $0.5\text{Li}_2\text{O}\cdot 0.5\text{Na}_2\text{O}\cdot\text{Al}_2\text{O}_3\cdot 2.0\text{SiO}_2$ Glass.....	35
11. Comparison of Internal Friction Experimental Data and Analytical Solution, $\text{Li}_2\text{O}\cdot\text{Al}_2\text{O}_3\cdot 2.0\text{SiO}_2$ Glass, Frequency 0.76 HZ.....	36
12. Comparison of Internal Friction Experimental Data and Analytical Solution, $0.5\text{Li}_2\text{O}\cdot 0.5\text{Na}_2\text{O}\cdot\text{Al}_2\text{O}_3\cdot$ 2.0SiO_2 Glass, Frequency 0.644 HZ.....	37
13. β Variation with Temperature, $\text{Li}_2\text{O}\cdot\text{Al}_2\text{O}_3\cdot 2.0\text{SiO}_2$ Glass.....	38
14. β Variation with Temperature, $0.5\text{Li}_2\text{O}\cdot 0.5\text{Na}_2\text{O}\cdot$ $\text{Al}_2\text{O}_3\cdot 2.0\text{SiO}_2$ Glass.....	39
15. β Variation with Frequency.....	40
16. Internal Friction Curve, $\text{Li}_2\text{O}\cdot\text{Al}_2\text{O}_3\cdot 2.0\text{SiO}_2$ Glass, Frequency 0.0734 HZ.....	57

LIST OF ILLUSTRATIONS (continued)

Figures	Page
17. Internal Friction Curve, $\text{Li}_2\text{O}\cdot\text{Al}_2\text{O}_3\cdot 2.0\text{SiO}_2$ Glass, Frequency 0.136 HZ.....	58
18. Internal Friction Curve, $\text{Li}_2\text{O}\cdot\text{Al}_2\text{O}_3\cdot 2.0\text{SiO}_2$ Glass, Frequency 1.20 HZ.....	59
19. Internal Friction Curve, $\text{Li}_2\text{O}\cdot\text{Al}_2\text{O}_3\cdot 2.0\text{SiO}_2$ Glass, Frequency 1933 HZ.....	60
20. Internal Friction Curve, $\text{Li}_2\text{O}\cdot\text{Al}_2\text{O}_3\cdot 2.0\text{SiO}_2$ Glass, Frequency 2571 HZ.....	61
21. Internal Friction Curve, $\text{Li}_2\text{O}\cdot\text{Al}_2\text{O}_3\cdot 2.0\text{SiO}_2$ Glass, Frequency 3293 HZ.....	62
22. Internal Friction Curve, $0.5\text{Li}_2\text{O}\cdot 0.5\text{Na}_2\text{O}\cdot\text{Al}_2\text{O}_3\cdot$ 2.0SiO_2 Glass, Frequency 0.0914 HZ.....	63
23. Internal Friction Curve, $0.5\text{Li}_2\text{O}\cdot 0.5\text{Na}_2\text{O}\cdot\text{Al}_2\text{O}_3\cdot$ 2.0SiO_2 Glass, Frequency 0.296 HZ.....	64
24. Internal Friction Curve, $0.5\text{Li}_2\text{O}\cdot 0.5\text{Na}_2\text{O}\cdot\text{Al}_2\text{O}_3\cdot$ 2.0SiO_2 Glass, Frequency 1.044 HZ.....	65
25. Internal Friction Curve, $0.5\text{Li}_2\text{O}\cdot 0.5\text{Na}_2\text{O}\cdot\text{Al}_2\text{O}_3\cdot$ 2.0SiO_2 Glass, Frequency 1756 HZ.....	66
26. Internal Friction Curve, $0.5\text{Li}_2\text{O}\cdot 0.5\text{Na}_2\text{O}\cdot\text{Al}_2\text{O}_3\cdot$ 2.0SiO_2 Glass, Frequency 2024 HZ.....	67
27. Internal Friction Curve, $0.5\text{Li}_2\text{O}\cdot 0.5\text{Na}_2\text{O}\cdot\text{Al}_2\text{O}_3\cdot$ 2.0SiO_2 Glass, Frequency 2751 HZ.....	68

LIST OF TABLES

Tables	Page
I. Operating Limits of Experimental Equipment.....	41
II. Internal Friction Data, $\text{Li}_2\text{O}\cdot\text{Al}_2\text{O}_3\cdot 2.0\text{SiO}_2$ Glass.....	42
III. Internal Friction Data, $0.5\text{Li}_2\text{O}\cdot 0.5\text{Na}_2\text{O}\cdot\text{Al}_2\text{O}_3\cdot 2.0\text{SiO}_2$ Glass.....	43
IV. Comparison of Internal Friction Data Before and After 48 Hour Heat Treatment.....	44
V. Distributions in Activation Entropy.....	45
VI. Correction of Peak Height for Relaxation Ratio, $\text{Li}_2\text{O}\cdot\text{Al}_2\text{O}_3\cdot 2.0\text{SiO}_2$ Glass.....	54
VII. Correction of Peak Height for Relaxation Ratio, $0.5\text{Li}_2\text{O}\cdot 0.5\text{Na}_2\text{O}\cdot\text{Al}_2\text{O}_3\cdot 2.0\text{SiO}_2$ Glass.....	55

I. INTRODUCTION

Internal friction is a measure of the damping or energy absorption of a material caused by some relaxation mechanism involving the atoms, the specific arrangement of the atoms, or the defect structure of the atoms. Internal friction and damping measurements have been utilized to study the submicro-, micro-, and macrostructure of crystalline materials and the mechanisms responsible for inelastic deformation⁽¹⁾. Rheological and damping measurements have also helped clarify the molecular structure and deformation mechanisms of polymers and elastomers⁽²⁾. Bibliographies⁽³⁻⁴⁾ and general references⁽⁵⁻⁷⁾ concerning internal friction, material damping, and other related areas have been published for crystalline materials as well as glasses. Previously internal friction techniques have been applied to glass to obtain information concerning the atomic structure of glass and the relaxation mechanisms involved in the internal friction.

In crystalline materials internal friction studies have yielded rather specific identification of the mechanisms causing the relaxation or energy absorption. In non-crystalline materials this identification has been less specific, partly because of the non-periodicity of the glass structure and partly because a common arrangement between glass systems isn't known. There are many crystalline materials with a face-centered cubic, hexagonal

close packed, and body-centered cubic arrangement of the atoms or molecules that have greatly different physical properties. This arrangement of the atoms creates a common factor or similarity among all of these materials. In non-crystalline materials this common factor is lacking.

Silicate⁽⁸⁻¹⁶⁾, aluminosilicate⁽¹⁷⁻¹⁸⁾, and borosilicate⁽¹⁹⁾ glasses have been more thoroughly studied in recent years by the internal friction technique than other non-crystalline materials. Several mechanisms have been proposed for the internal friction peaks observed in these glasses. The proposed mechanisms include the stress-induced movement of alkali ions in alkali containing glasses^(8,9,20-22), a cooperative motion of dissimilar alkali ions in mixed alkali glasses^(14,18,23), and a movement of non-bridging oxygen ions in those glasses containing non-bridging ions^(9,17,20,24). Ryder and Rindone⁽²⁴⁾ showed that the addition of alkaline-earth ions to an alkali silicate glass causes a change in the magnitude and temperature of the alkali peak. They also present data for a $0.25\text{CaO}\cdot 0.75\text{BaO}\cdot 2.0\text{SiO}_2$ glass which had a small internal friction peak, but do not give an explanation for it. Later Graham and Rindone⁽²⁵⁾ showed that ice on the surface of a fiber caused an internal friction peak in a $\text{BaO}\cdot 2.0\text{SiO}_2$ glass. Unless ice is present no peak is observed in this glass between -170°C and 23°C . The water content⁽²⁶⁾, the number of proton ions⁽²⁷⁾, and the degree of phase separation⁽²⁸⁾ have all been proposed as affecting the

internal friction. Taylor⁽¹⁶⁾ recently reported that changing the amount of phase separation did not change the internal friction for a mixed lithium-sodium glass.

In a material containing many relaxing units, each unit has a characteristic relaxation time. Since the arrangement of the atoms is not perfect, there generally exists a distribution of relaxation times for any one type of relaxation mechanism. Because of the greater disorder in glasses the distribution of relaxation times is much wider than in crystalline materials⁽²⁹⁻³⁰⁾. For a thermally activated relaxation mechanism the relaxation time is given by the Arrhenius equation

$$\tau = \tau_0 \exp \left\{ \frac{E_a}{RT} \right\} = \frac{h}{kT} \exp \left\{ - \frac{\Delta S}{R} \right\} \exp \left\{ \frac{E_a}{RT} \right\} \quad (1)$$

τ = Relaxation time for a particular process

τ_0 = Pre-exponential term

h = Planck's constant

k = Boltzmann's constant

T = Temperature, °K

ΔS = Activation entropy

R = Gas constant

E_a = Activation energy

A distribution in relaxation times can be caused by a distribution in the pre-exponential term, which is related to the activation entropy, or in the activation energy.

Extensive studies⁽³¹⁻³³⁾ of the distribution of relaxation times for crystalline materials have helped to explain the relaxation mechanism and the defect structure of the material. Internal friction peaks in glasses are known to exhibit a considerably wider distribution of relaxation times than crystalline materials but the character of the distribution has not been thoroughly studied except for the work of Ferry⁽⁸⁾ and Copley and Oakley⁽²⁹⁾ dealing with the alkali peak. It hasn't been reported for glasses whether the width of the distribution is caused by the pre-exponential term or the activation energy, although most discussions have centered on the activation energy.

This study was undertaken to analyze the distribution of relaxation times for both the alkali and the mixed alkali peak. There has been no previous work on the mixed peak since it was just recently reported. A lithium aluminosilicate and a lithium-sodium aluminosilicate glass were selected for study since the peaks are large and well resolved from a low background that remains practically constant over a wide temperature range. The internal friction in these two glasses is attributed to different relaxation mechanisms, as will be explained in more detail later. The analysis of the experimental data and the comparison to the analytical solution based on an assumed distribution of relaxation times yields information

regarding the symmetry of the distribution, the distribution of activation entropies, and the distribution of activation energies.

II. EXPERIMENTAL PROCEDURE

A. Sample Preparation

The glasses studied were $\text{Li}_2\text{O}\cdot\text{Al}_2\text{O}_3\cdot 2.0\text{SiO}_2$ and $0.5\text{Li}_2\text{O}\cdot 0.5\text{Na}_2\text{O}\cdot\text{Al}_2\text{O}_3\cdot 2.0\text{SiO}_2$. The batch materials for the single and mixed alkali glass were chemically pure Li_2CO_3 and Al_2O_3 and certified grade Li_2CO_3 , Na_2CO_3 , and Al_2O_3 , respectively. Potters flint (99.98% SiO_2) was used for both glasses. Approximately 0.03 weight percent of NaI was added to the mixed alkali glass to promote fining in the melt. The chemical analysis of all ingredients is shown in Appendix A.

Prior to melting, the batch materials were wet mixed with certified grade acetone to assure homogeneity and dried. The glasses were melted in platinum crucibles for approximately eight hours at 1500-1550°C in an electric furnace open to the atmosphere. Two glass bars were formed in a stainless steel mold, 1/4 in. x 1/2 in. x 6 in., and several feet of glass fibers, approximately 0.5 mm diameter, were drawn from the same bubble-free melt. To insure a uniform thermal history, the fibers and glass bars were annealed simultaneously in an electric furnace. The annealing cycles are shown in Figures 1 and 2. A transmission polariscope was used to determine that the annealed bars were free of the residual stress induced by the initial cooling cycle.

B. Internal Friction Measurements

A resonance technique based on Forster's⁽³⁴⁾ method of suspension (sonic damping equipment) was used to determine the internal friction of a bar vibrating in flexure in a free-free mode. A block diagram of the equipment, identical to that described by Taylor⁽¹⁶⁾, is shown in Figure 3. The temperature of the specimen was determined by four Chromel-Alumel thermocouples embedded in a glass bar of approximately the same dimensions as the specimen bar. The thermocouple bar was located in the same position with respect to the specimen, the furnace wire coils, and the sides of the cooling chamber on each measurement to enable comparison of the data between different measurements. The internal friction of the specimen was calculated using equation (2).

$$Q^{-1} = \frac{1}{n\pi} \ln(\text{Amplitude ratio}) \quad (2)$$

$$Q^{-1} = \text{Internal friction}$$

$$n = \text{Number of cycles}$$

Amplitude ratio is ratio of amplitude on zeroth cycle and on nth cycle of vibration

By changing the physical dimensions of the glass bar, measurements were obtained at several different frequencies.

The torsion pendulum shown schematically in Figure 4 was similar to that described previously^(14,35). Temperatures were measured using three Chromel-Alumel thermocouples along the length of the glass fiber. The internal friction

of the fiber was calculated from equation (2). By changing the length of the fiber and repositioning the weights on the inertia bar, measurements on the pendulum were made at different resonant frequencies.

All internal friction measurements were made in a vacuum chamber to minimize air damping. Elevated temperatures were obtained with nichrome wire heating elements while liquid nitrogen was used to cool the specimen below room temperature. Table I shows the operating limits applicable to both pieces of equipment.

C. Activation Energy

A thermally activated relaxation mechanism has a relaxation time as given by the Arrhenius equation. Since at the peak temperature $\omega\tau = 1$ and $\omega = 2\pi f$ then

$$\frac{1}{2\pi f} = \tau_0 \exp \left\{ \frac{E_a}{RT} \right\} \quad (3)$$

f = Frequency of oscillation of internal friction peak

As the resonant frequency is changed the peak temperature also changes and the activation energy for the relaxation mechanism can be calculated from the equation

$$E_a = R \frac{\ln f_1 - \ln f_2}{\frac{1}{T_2} - \frac{1}{T_1}} \quad (4)$$

T = Internal friction peak temperature, $^{\circ}\text{K}$

Several data points obtained on the torsion pendulum and the sonic damping equipment were used, with a least squares

approximation to a straight line, to determine the activation energy of the relaxation mechanism in each glass.

III. RESULTS

Typical internal friction versus temperature curves for the two glasses are shown in Figures 5 and 6. The internal friction peaks shown in Figure 5 for the $\text{Li}_2\text{O} \cdot \text{Al}_2\text{O}_3 \cdot 2.0\text{SiO}_2$ glass are explained as follows. The large peak at -27°C is attributed to a stress induced movement of the predominant alkali ion, lithium. The two much smaller peaks at 170°C and 350°C could be due to one of the following: (1) a small amount of sodium or potassium alkali ions introduced into the glass as impurities in the raw materials, (2) a small number of non-bridging oxygen ions if the alkali to aluminum ratio isn't exactly one, (3) a small amount of water, hydroxol group, or proton. Precautions were taken to minimize any effect caused by the above factors. The impurity alkali content was minimized (see Appendix A) in the $\text{Li}_2\text{O} \cdot \text{Al}_2\text{O}_3 \cdot 2.0\text{SiO}_2$ glass, particularly the amount of sodium since Day and Steinkamp⁽¹⁸⁾ reported that even 0.005 mole percent of the second alkali caused a noticeable internal friction peak. The raw materials were weighed on an electric analytical balance to an accuracy of ± 0.001 grams to help insure that the actual composition of the glass was as close as possible to the stated composition. All the raw materials, with the exception of the silica, were kept in closed containers, the batch was kept in a drying oven before being placed in a furnace, and all specimens were kept in desiccators before being

tested. These small peaks had no effect upon the results of this study, i.e., the distribution of relaxation times in the large peak, and do not warrant further consideration.

In the internal friction curve for the mixed alkali glass, $0.5\text{Li}_2\text{O}\cdot 0.5\text{Na}_2\text{O}\cdot \text{Al}_2\text{O}_3\cdot 2.0\text{SiO}_2$, shown in Figure 6, only one large peak was observed.

Comparisons of the data obtained with the torsion pendulum and the sonic damping equipment are shown in Figures 7 and 8. The background has been subtracted so only the net internal friction is shown. A linear expression was used for the background of the aluminosilicate glasses, based on the internal friction values on the low and high temperature sides of the peak, since the apparent background remains practically constant (see Figures 5 and 6). The good agreement between the individual peak heights with the fiber in torsion and the bar in flexure is explained in detail in Appendix B.

The peak temperatures and heights above background for the two glasses are shown in Tables II and III. The change in peak temperature with frequency, yielding the activation energy for the relaxation mechanism, for both glasses is shown in Figures 9 and 10. The least squares determination of the activation energy is within ± 1 kcal/mole when allowing a $\pm 5^\circ\text{C}$ variation in the peak temperatures measured

on the sonic damping equipment and a $\pm 2^{\circ}\text{C}$ variation on those measured on the torsion pendulum.

It will be shown later that a narrow distribution of activation energies exists in these two glasses. Since the distribution is narrow a single value for the activation energy can be used in equation (1) without significant error^(19,36). Using the most probable value of the activation energy and equation (1), the internal friction versus temperature plot can be converted to an internal friction versus relaxation time plot. Figures 11 and 12 show typical data for both glasses plotted against the relaxation time with the internal friction values normalized so the peak value is 1.0. The data for the other measurements taken in this study are shown in Appendix C.

In order to determine whether adsorbed water might change the internal friction the following experiment was completed. A bar of the $\text{Li}_2\text{O}\cdot\text{Al}_2\text{O}_3\cdot 2.0\text{SiO}_2$ glass was held at approximately 425°C for 48 hours in a vacuum in the sonic damping equipment and cooled to room temperature. The bar was then cooled to -120°C and heated to above room temperature in the normal manner. As shown in Table IV, this heat treatment caused no significant difference in the internal friction.

IV. DISCUSSION

A. Relaxation Time Distribution Function

A distribution in relaxation times (eq.(1)) can be caused by a distribution in τ_0 , which implies a distribution in the activation entropy, or a distribution in the activation energy. A distribution function $K(\tau)$ applied to the equation obtained by Debye for an energy absorption with a single relaxation time gives

$$Q^{-1} = \Delta \int_0^{\infty} K(\tau) \frac{\omega \tau}{1 + \omega^2 \tau^2} d\tau \quad (5)$$

Δ = Relaxation ratio

$K(\tau)$ = Assumed distribution function

$\omega = 2\pi f$ = Angular frequency

f = Linear frequency

τ = Relaxation time

Several distribution functions were considered in this study. A Cauchy distribution in the variable τ gave an unsymmetrical expression for Q^{-1} , which appears appropriate from the experimental data, but the calculated values were high on the low $\omega\tau$ side of the peak, rather than on the high $\omega\tau$ side. A uniform distribution in τ and in $\ln\tau$ was considered, but the calculated values were too narrow for the experimental peak. A Cauchy distribution in $\ln\tau$ gave a symmetrical curve as did the normal distribution in $\ln\tau$ (lognormal distribution). The Cauchy distribution in $\ln\tau$ and the lognormal distribution gave considerably better agreements than any of the others and

in the region of the maximum the lognormal provided the best agreement with the experimental data. Hence, the lognormal distribution of relaxation times has been used in the analysis of the data.

It was mentioned previously that all known relaxation mechanisms in solids have a distribution of relaxation times rather than a single relaxation time. In crystalline materials the mechanisms have a relatively narrow distribution of relaxation times. For narrow distributions Nowick and Berry⁽³⁰⁾ report no noticeable difference between a uniform distribution and a lognormal distribution. However, they state that this would not be true for a wide distribution of relaxation times, which is the case for glasses.

The lognormal distribution function is

$$K(\tau) d\tau = \frac{1}{\beta\sqrt{\pi}} \exp \left\{ -z^2/\beta^2 \right\} dz \quad (6)$$

$$z = \ln \tau / \tau_m$$

τ_m = Mean value of relaxation time

β is related to the half-height peak width of the lognormal distribution

The result of substituting equation (6) in equation (5) is

$$Q^{-1}(X, \beta) = \frac{\Delta}{2\sqrt{\pi}} \int_{-\infty}^{\infty} \exp \left\{ -U^2 \right\} \operatorname{sech} (X + \beta U) dU \quad (7)$$

$$X = \ln \tau_m$$

U = Dummy variable under the integral sign

Some of the mathematical steps between equations (5) and (7) are shown by Nowick and Berry⁽³⁷⁾. The entire derivation is presented in Appendix D. The analytical expression for internal friction based on the lognormal distribution of relaxation times is compared with the experimental data in Figures 11 and 12. The curves based on the lognormal distribution are a ratio of the $Q^{-1}(x, \beta)/Q^{-1}(0, \beta)$ obtained from equation (7). A numerical integration technique on an IBM 360 computer was used to evaluate equation (7).

The experimental internal friction along with the analytical solution based on the lognormal distribution shown in Figure 12 provides the first known comparison for a mixed alkali glass. There is reasonably good agreement with the lognormal distribution and it appears that the distribution of relaxation times in the $0.5\text{Li}_2\text{O}\cdot 0.5\text{Na}_2\text{O}\cdot \text{Al}_2\text{O}_3\cdot 2.0\text{SiO}_2$ glass is very close to being lognormal. The area under the experimental curve and the curve based on the analytical solution was determined. In all measurements for the $0.5\text{Li}_2\text{O}\cdot 0.5\text{Na}_2\text{O}\cdot \text{Al}_2\text{O}_3\cdot 2.0\text{SiO}_2$ glass the experimental curve enclosed 1.05 ± 0.04 more area than the curve based on the lognormal distribution. In all cases the ratio remained relatively constant.

Figure 11 makes a similar comparison for the $\text{Li}_2\text{O}\cdot \text{Al}_2\text{O}_3\cdot 2.0\text{SiO}_2$ glass. In this glass the experimental curve enclosed 1.24 ± 0.04 more area than the analytical

curve, with the ratio remaining relatively constant for individual measurements. In comparing the experimental data to the analytical solution based on the lognormal distribution it is seen that at high $\omega\tau$ values (low temperature side of the peak) the experimental data is considerably higher than the analytical solution yields for both glasses. Copley and Oakley⁽²⁹⁾ reported similar results for the alkali peak in sheet glass and Forry's⁽⁸⁾ work essentially shows the same trend even though the lowest temperature investigated in his work was -90°C .

The lognormal distribution function will be used to analyze the distribution of relaxation times for the internal friction peaks since it provides the best agreement with the experimental data. The agreement for the mixed alkali glass is more than adequate over almost the entire temperature range investigated. The agreement of the lognormal distribution for the single alkali glass is less than in the mixed alkali glass but it allows for reasonable interpretations of the data.

B. Long Tail of the Experimental Data

The experimental data of both glasses have a "long drawn out tail" at high $\omega\tau$ values. Any symmetrical distribution function will not compare favorably in this region. This same situation has been observed by Copley and Oakley⁽²⁹⁾. They suggest that this long tail might be caused by the presence of water in the specimen.

The precautions taken to minimize the water content of the glass have been previously stated. Table IV shows the comparison of data for two measurements on the same bar, where another precaution was taken to eliminate any surface water. The comparison of the data regarding peak height, peak frequency, peak temperature, and peak width at half-height shows no significant change. The first measurement was made in the normal manner, while in the second the bar was held at approximately 425°C for 48 hours under vacuum before the internal friction was measured. There was a period of several days between measurements when the bar was in a desiccator. It is expected, that the 48 hour heat treatment would be sufficient to remove any water adsorbed on the glass surface. If adsorbed water was the cause of the long tail then some change should have been observed.

In both glasses the experimental values are higher than the symmetric lognormal distribution would predict at the large $\omega\tau$ values. When comparing $\pm X'$ values the higher experimental value for the positive X' indicates that more units are relaxing at a lower energy level ($+X'$, low temperature) than are relaxing at the higher energy level ($-X'$, higher temperature). This would be expected, since it should be easier and more probable, that the units possessing the lower energy levels would participate before those having the higher energy levels. The random arrangement of ions probably form units which

possess a symmetrical distribution of energy levels, but the lower levels are those that are broken first, easiest, and with the greatest probability.

C. β Variation with Temperature

The β parameter in equation (7) describes the width of the lognormal distribution. Nowick and Berry (30) show that β is related to the distribution in τ and that it is possible to separate the effect of a distribution in τ_0 from a distribution in the activation energy. An equation of the following form is obtained

$$\beta = \beta_0 + \frac{\beta_E}{RT} \quad (8)$$

β_0 is related to the distribution in τ_0 .

β_E is related to the distribution in the activation energy.

The above equation is that of a straight line when β is plotted versus $1/T$; β_0 is the intercept value and β_E is determined from the slope. Figures 13 and 14 show the temperature variation in β for both glasses. Shown with each data point in these figures are the reasonable variations that might be expected. The peak temperature reproducibility has been listed in Table I. The tolerances in the β values are based on a $\pm 1^\circ\text{C}$ deviation in the temperatures used to calculate the peak width. Both of these variations are stated in Tables II and III with the peak widths and β values.

The temperature variation in β indicates a change in the distribution of relaxation times with temperature. Kirby⁽¹⁹⁾ states "It appears that the width of the distribution of relaxation periods does not vary greatly with temperature". This statement is based on data from low-frequency torsion pendulum measurements, although one measurement obtained by Marx and Sivertsen⁽³⁸⁾, was reported at a frequency of 37 khz. It is not possible to determine from Kirby's work any variation in β with temperature. The temperature variation of β , as shown in Figures 13 and 14, is larger than anything previously reported. The frequency range covered in this study was from 0.07 hz. to 3293 hz. Over this frequency range a larger variation in β would occur than over the limited frequency range of the torsion pendulum. Kirby⁽¹⁹⁾ also reports "A similar result has been noted by H. E. Taylor⁽³⁹⁾ in the case of the dielectric relaxation attributable to the same class of ion", indicating that Taylor also found that the distribution of relaxation times doesn't change considerably with temperature. The frequency of Taylor's work wasn't reported. These two studies specifically concerned sodium ions in "Pyrex" glass, however, it is felt that sodium and lithium should cause similar distributions of relaxation times.

D. Distribution in Activation Energy and Activation Entropy

The distribution in τ_0 , meaning the activation entropy, and the activation energy are obtained from the least squares determination of the linear fit to the data points in Figures 13 and 14. When the β_0 and β_E values are determined from these figures it is found that the distribution in τ_0 , or the activation entropy, is the same in the mixed alkali glass as in the single alkali glass. This is surprising since the proposed relaxation mechanisms are different, i.e., in the single alkali glass the proposed mechanism is a stress-induced motion of a single alkali ion and in the mixed alkali glass the proposed mechanism is a cooperative movement of two dissimilar alkali ions. Nothing has been reported regarding the similarity of order or disorder or the variation of order or disorder in a single alkali or mixed alkali glass.

Using equation (1) the activation entropy for the relaxation mechanism can be determined from the calculated value of τ_0 . For the single alkali glass and the mixed alkali glass the calculated average values of the activation entropy are respectively, 6.7 and 7.7 ± 0.5 cal/mole^oK. The values are comparable to those reported by Kirby⁽¹⁹⁾ for a "Pyrex" glass of 4.4 cal/mole^oK, by Shelby⁽⁴⁰⁾ for lithium-sodium silicate glasses of approximately 7.0 cal/mole^oK, and by McVay⁽⁴¹⁾ for sodium-rubidium silicate glasses of approximately 5.4 cal/mole^oK. The activation

entropy term should give an indication of the disorder in the structure in the environment of the ions participating in the relaxation mechanism. If we consider the relaxation mechanism as a unit moving against an energy barrier a change in the activation entropy term can be interpreted as a change in the shape of the barrier. Likewise a change in the activation energy term can be regarded as a change in the height of the barrier. Thus it is noted that in this study the measure of disorder is slightly higher in the mixed alkali glass than in the single alkali glass, but the values obtained here and those reported elsewhere for a wide variation in compositions are remarkably similar. Thus it appears that the alkali ions don't significantly change the disorder that exists within the structure, at least the disorder around the ions or units that participate in the relaxation doesn't vary significantly for different alkali ions.

The β parameter is related to the standard deviation (σ) of the lognormal distribution. Using normal distribution tables and the known standard deviation value the spread of values that includes some predetermined percent of values can be calculated. A spread of approximately $\pm 2\sigma$ will include 95 percent of the values in a lognormal distribution. This percentage has been used throughout this study. Table V shows data concerning the activation entropy and the range of values based on a lognormal

distribution. It is seen that a spread of ± 3.1 cal/mole^oK around the average value of the activation entropy includes 95 percent of all the values in the distribution. The spread of activation entropies is obtained from the β_0 term explained in equation (8). To have a distribution of relaxation times, where there is no spread in the activation entropy, the intercept value in Figures 13 and 14 would have to be zero. Based on the data obtained for these two glasses this situation could not occur. Nowick and Berry⁽³⁰⁾ reported a β_0 of 0.32 for a Ag-Zn crystalline material, which corresponds to a spread in the activation entropy of ± 0.44 cal/mole^oK. They state that this is based on a very limited amount of data but it does allow a comparison between the variation of the activation entropy in a crystalline material with that occurring in glass.

The slope of the β versus $1/T$ plot in Figure 14 for the mixed alkali glass is slightly higher than for the single alkali glass in Figure 13, which implies that there is a broader distribution of activation energies in the mixed glass than in the single alkali glass. The average value of the activation energy is higher for the mixed glass than for the single alkali glass. Based on an assumed lognormal distribution of activation energies, the value of 15.3 kcal/mole for the single alkali glass, and the β_E value of 955 cal/mole from Figure 13, it can be calculated that 95 percent of the values of the activation energy

are between 14.0 and 16.6 kcal/mole (15.3 ± 1.3 kcal/mole). This narrow distribution supports the previous statement of using a single value of the activation energy in the Arrhenius equation. The same method of analysis yields for the $0.5\text{Li}_2\text{O} \cdot 0.5\text{Na}_2\text{O} \cdot \text{Al}_2\text{O}_3 \cdot 2.0\text{SiO}_2$ glass, the values of 22.3 ± 1.8 kcal/mole (20.5 to 24.1 kcal/mole).

It is concluded from this work, that the predominant contributor to the distribution of relaxation times is the wide distribution of activation entropies. The distribution of activation energies is narrow and has only a slight effect on the distribution of relaxation times.

Shelby⁽⁴⁰⁾ and McVay⁽⁴¹⁾ have reported in mixed alkali silicate glasses that the width of the distribution stays approximately the same for different composition ratios when the same two alkalis are mixed in different proportions. The data for both studies was obtained on the torsion pendulum and neither examined the variation in width of the distribution versus temperature for one composition.

Copley and Oakley⁽²⁹⁾ studied the alkali internal friction peak in sheet glass at various heat treat stages. Essentially they were changing the structure of the glass from the "as drawn" or chilled state to an annealed state. They reported an increase in the activation energy of the relaxation mechanism, a movement of the internal friction peak to higher temperatures, and an increase in the

distribution of relaxation times as the glass was progressively heat treated. They ran two different experiments, one involved heat treating at varying temperatures, stabilisation temperatures as they were called, and the other involved heat treating at 500°C for increasing periods of time. Approximately the same results were obtained in both experiments. They have observed an effect of the structure of the glass on the distribution of relaxation times while in this study the temperature variation of the distribution of relaxation times was obtained. Based on their reported data the structure caused a much larger change in the β parameter than does temperature and there appears to be a much larger distribution of activation energies than has been found in this study.

Using Figures 9 and 13 for the $\text{Li}_2\text{O}\cdot\text{Al}_2\text{O}_3\cdot 2.0\text{SiO}_2$ glass and Figures 10 and 14 for the $0.5\text{Li}_2\text{O}\cdot 0.5\text{Na}_2\text{O}\cdot\text{Al}_2\text{O}_3\cdot 2.0\text{SiO}_2$ glass a plot of β versus frequency can be obtained. These data, plotted in Figure 15, show that the lines for both glass compositions are essentially coincident, within experimental accuracy. This seems to imply that the relaxation mechanisms occurring in both glasses are related. A cooperative movement of dissimilar alkali ions in the mixed alkali glass and an alkali ion pair motion in the single alkali glass are two relaxation mechanisms that would satisfy the experimental data. In the mixed glass, with dissimilar alkali ions, there must exist bonds of

different strengths. For a unit to participate in the relaxation these bonds must be broken or stretched. It seems likely that this relaxation process would require a higher activation energy than the case where all bonds were equal. Also the disorder would probably be greater for dissimilar ions. Both of these situations occur. When the testing frequency is the same, the internal friction peak occurs at a higher temperature in the mixed glass than in the single alkali glass, because the activation energy is higher in the mixed alkali glass than in the single alkali glass. However, when the temperature parameter is eliminated, as in Figure 15, and a comparison made only between β and frequency the results appear coincident.

V. CONCLUSIONS

It has been determined that the lognormal distribution of relaxation times provides the best agreement with the experimental internal friction data. The agreement is better for the mixed alkali peak in a $0.5\text{Li}_2\text{O}\cdot 0.5\text{Na}_2\text{O}\cdot \text{Al}_2\text{O}_3\cdot 2.0\text{SiO}_2$ glass than for the alkali peak in a $\text{Li}_2\text{O}\cdot \text{Al}_2\text{O}_3\cdot 2.0\text{SiO}_2$ glass.

The β parameter varies with temperature, indicating a distribution in both the activation energy and the activation entropy. The temperature variation for β in the alkali aluminosilicate glasses is considerably larger than has been reported previously. It is felt that a similar study of other silicate and/or aluminosilicate glasses over a wide frequency range would also show a variation with temperature.

The major contribution to the distribution of relaxation times comes from a distribution in the activation entropy. The disorder and the variation in the disorder is considerably greater than in crystalline systems, while the disorder in various types of silicate glasses seems to be rather constant.

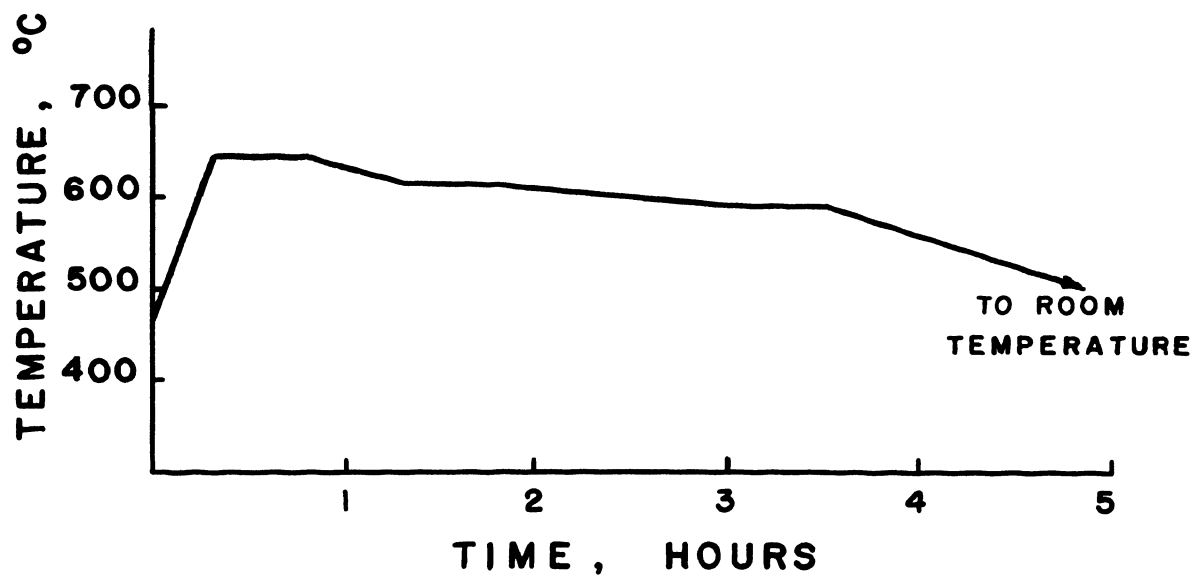


Figure 1. Annealing Cycle, $\text{Li}_2\text{O}\cdot\text{Al}_2\text{O}_3\cdot 2.0\text{SiO}_2$ Glass

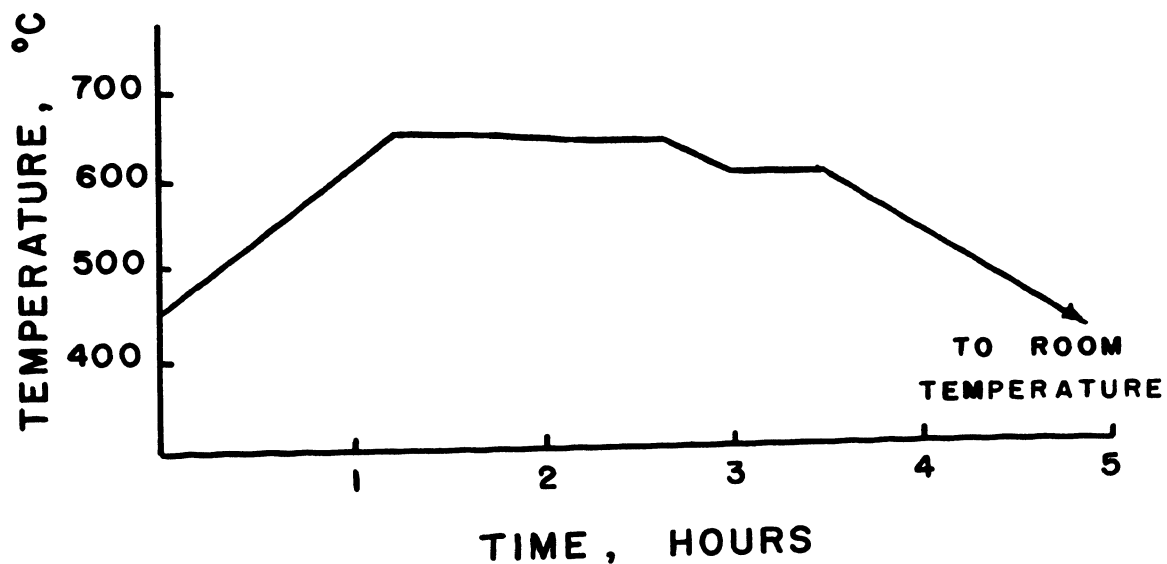


Figure 2. Annealing Cycle, $0.5\text{Li}_2\text{O}\cdot 0.5\text{Na}_2\text{O}\cdot\text{Al}_2\text{O}_3\cdot 2.0\text{SiO}_2$ Glass

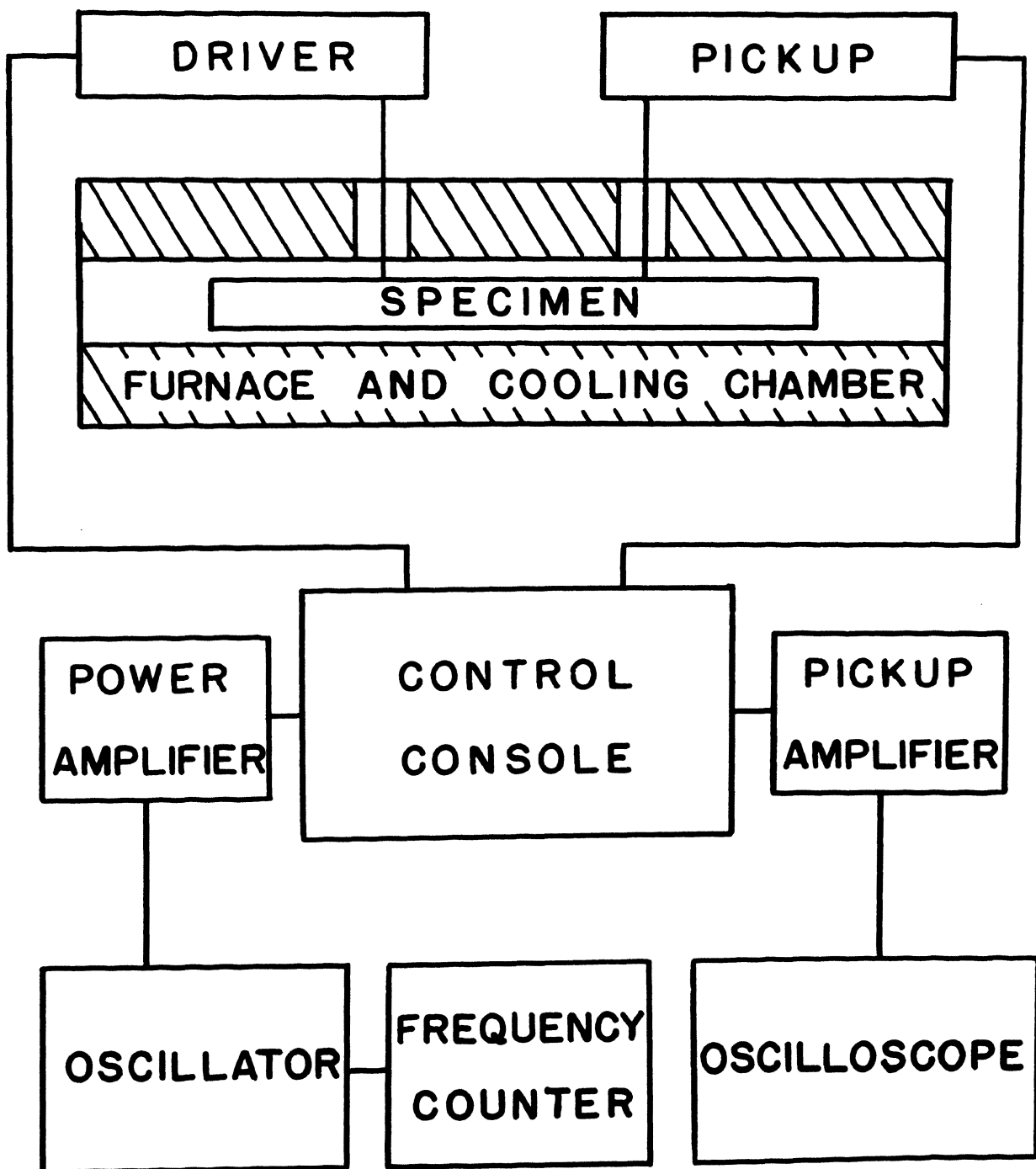


Figure 3. Block Diagram of Sonic Damping Equipment

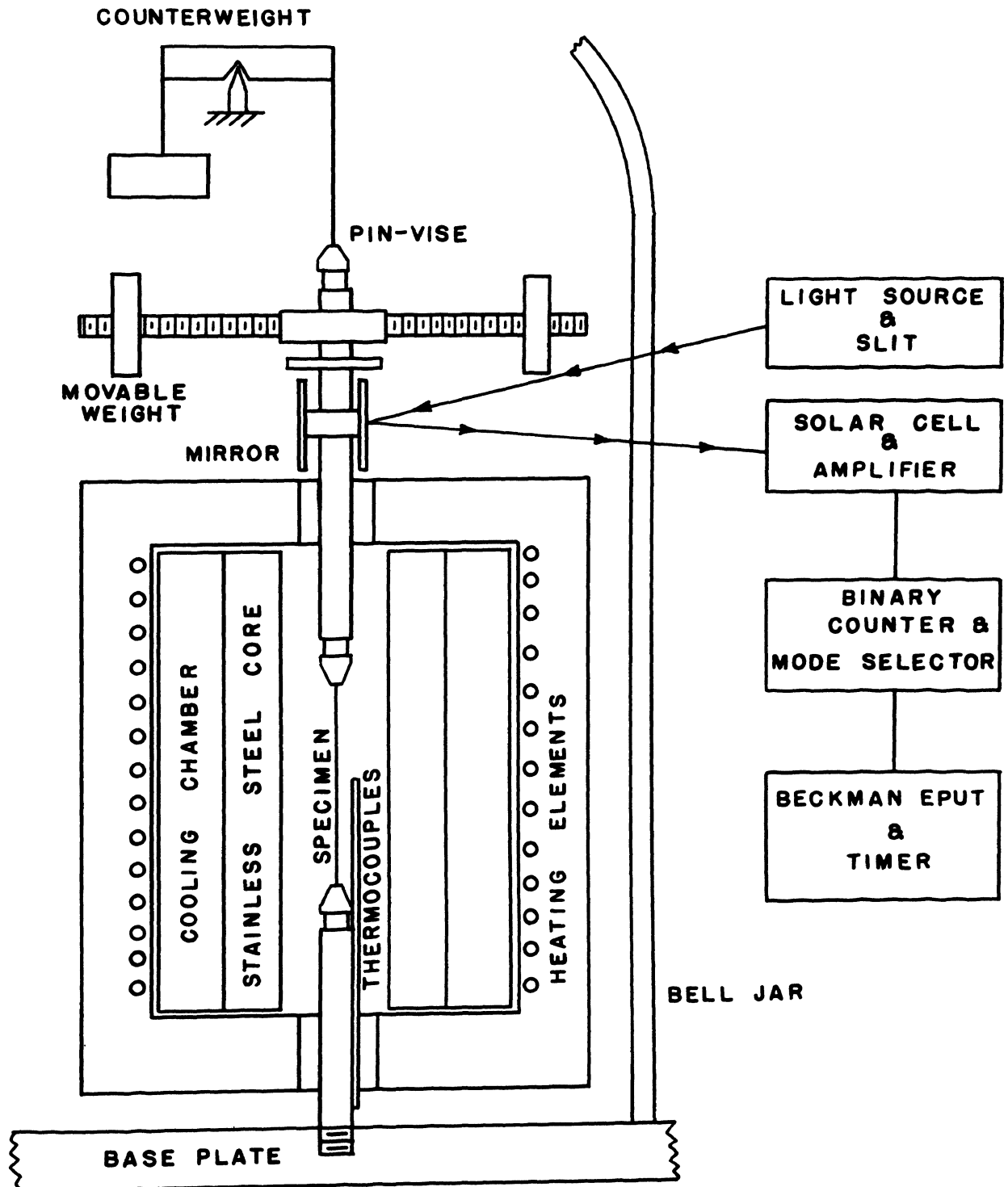


Figure 4. Schematic Diagram of Torsion Pendulum

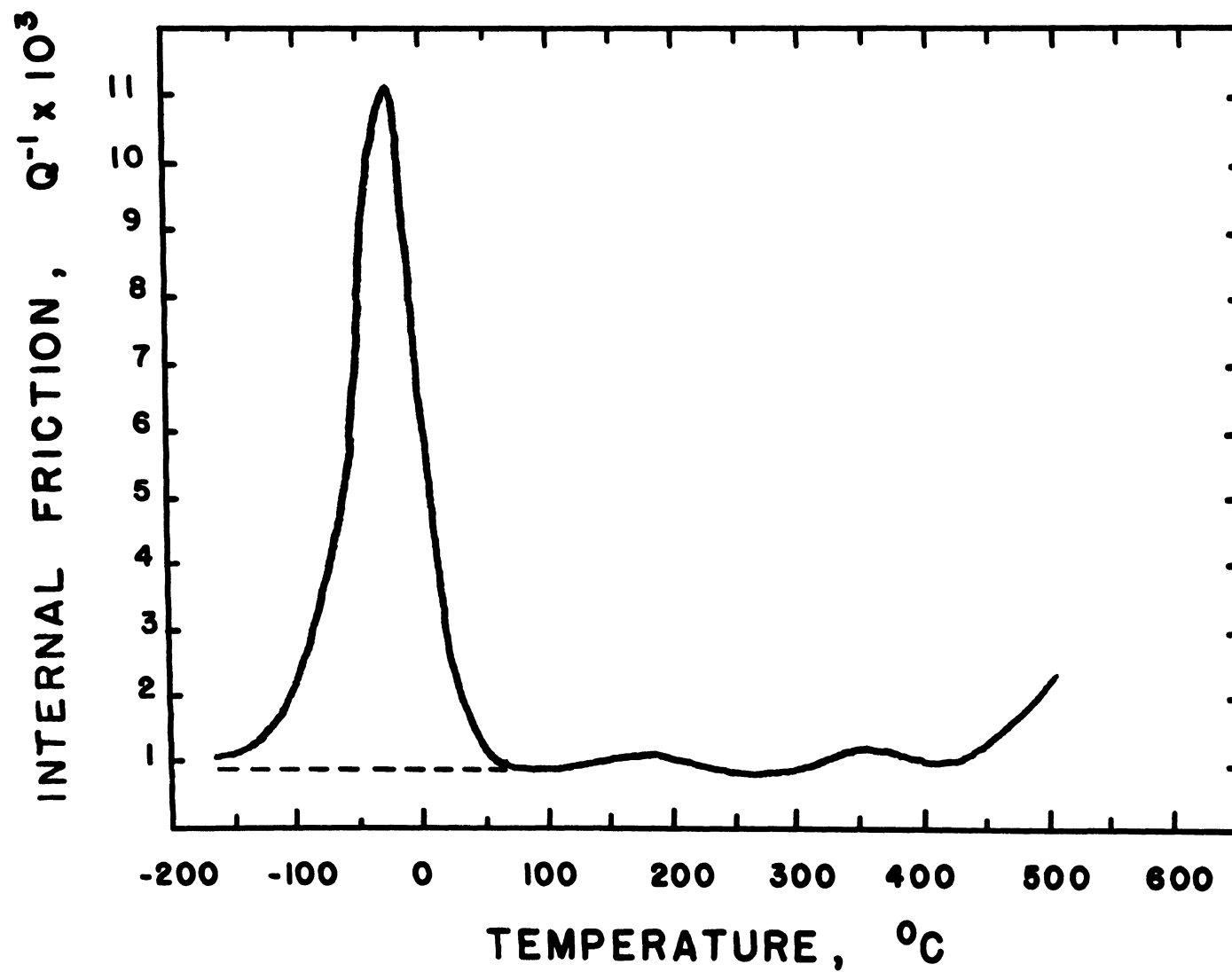


Figure 5. Typical Internal Friction Curve, $\text{Li}_2\text{O}\cdot\text{Al}_2\text{O}_3\cdot 2.0\text{SiO}_2$ Glass, Frequency 0.76 HZ.

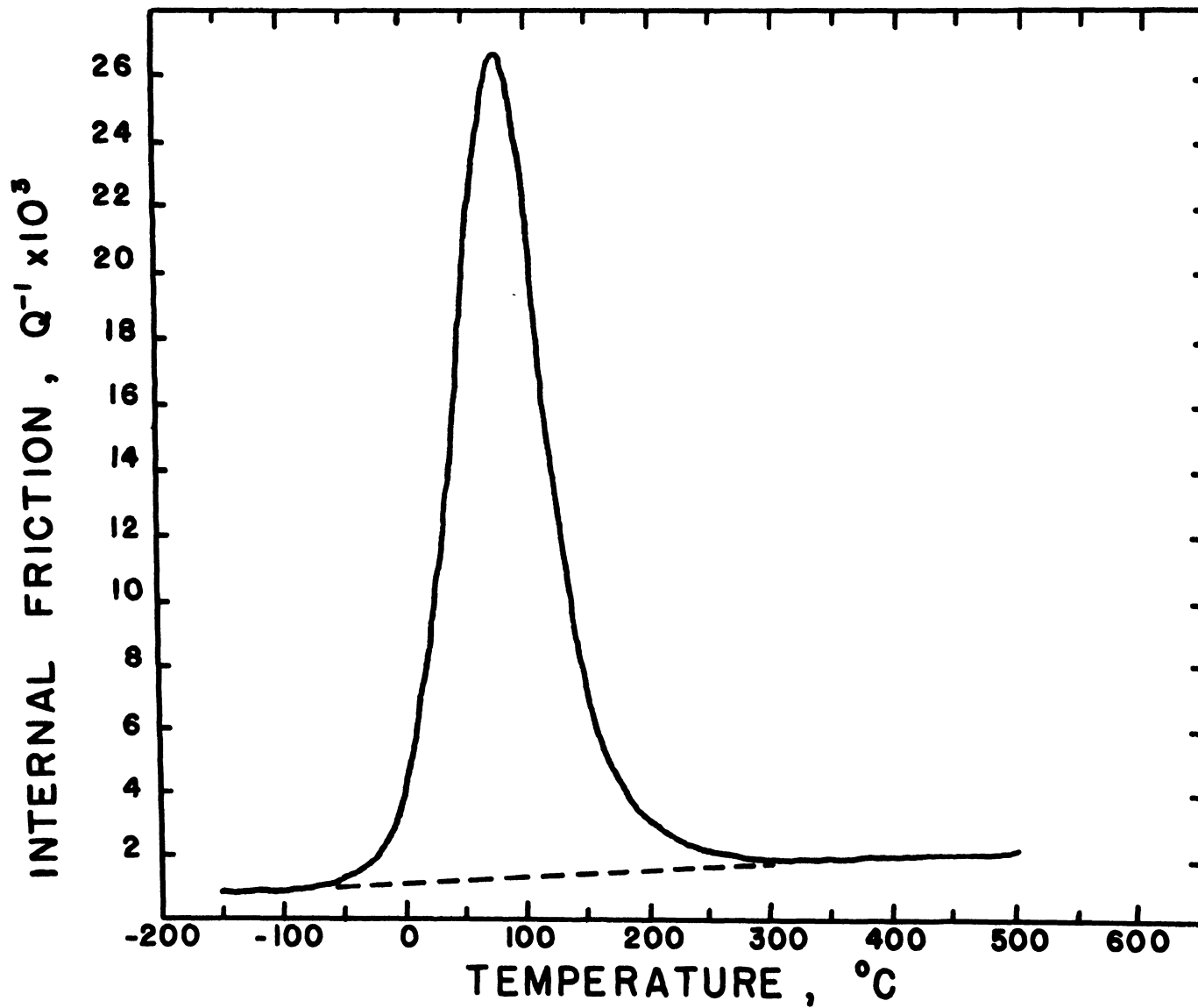


Figure 6. Typical Internal Friction Curve, $0.5\text{Li}_2\text{O} \cdot 0.5\text{Na}_2\text{O} \cdot \text{Al}_2\text{O}_3 \cdot 2.0\text{SiO}_2$ Glass, Frequency 0.644 HZ.

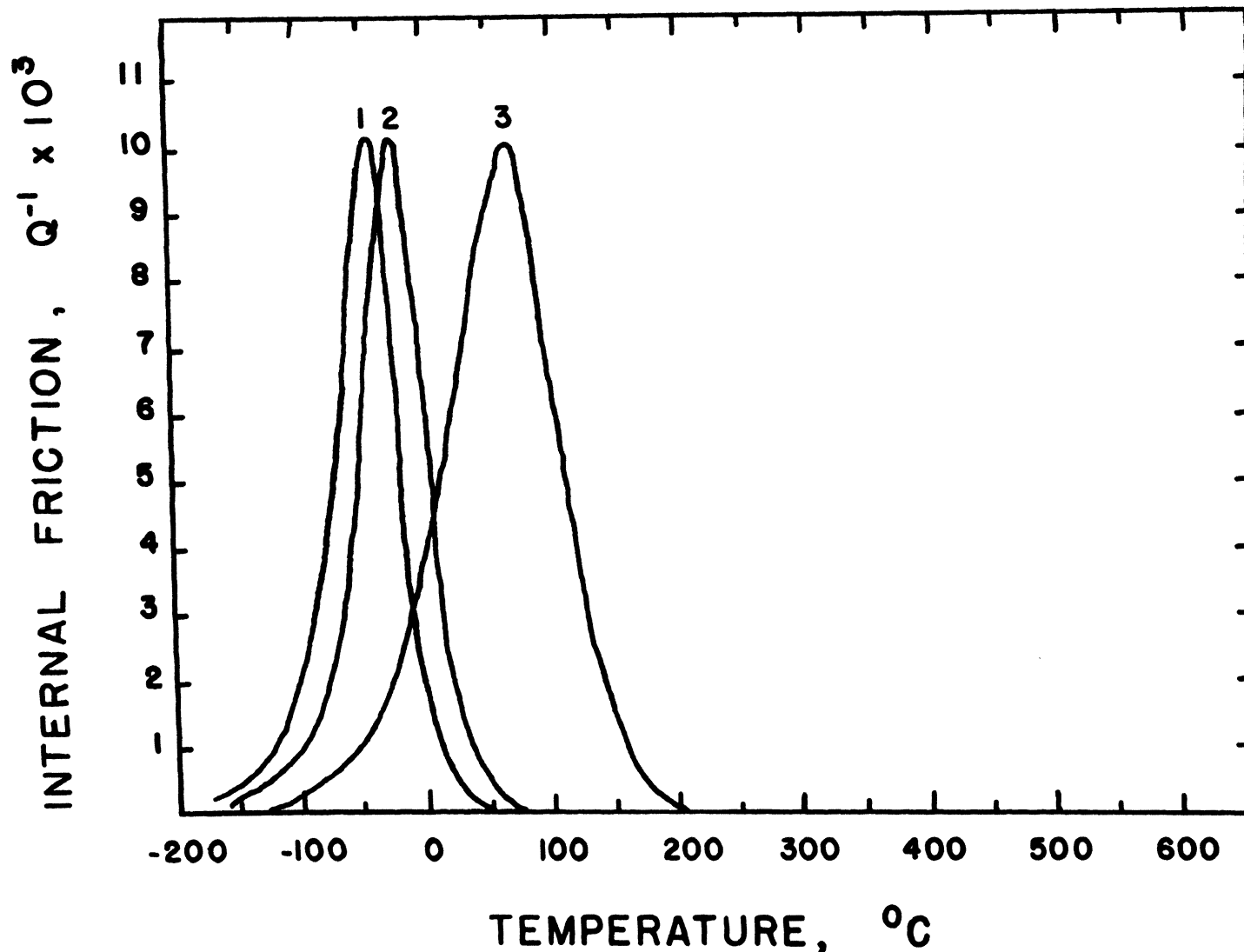


Figure 7. Comparison of Internal Friction Data on Torsion Pendulum and Sonic Damping Equipment, $\text{Li}_2\text{O} \cdot \text{Al}_2\text{O}_3 \cdot 2.0\text{SiO}_2$ Glass, Frequency (1) 0.0734 HZ., (2) 1.20 HZ., (3) 3293 HZ.

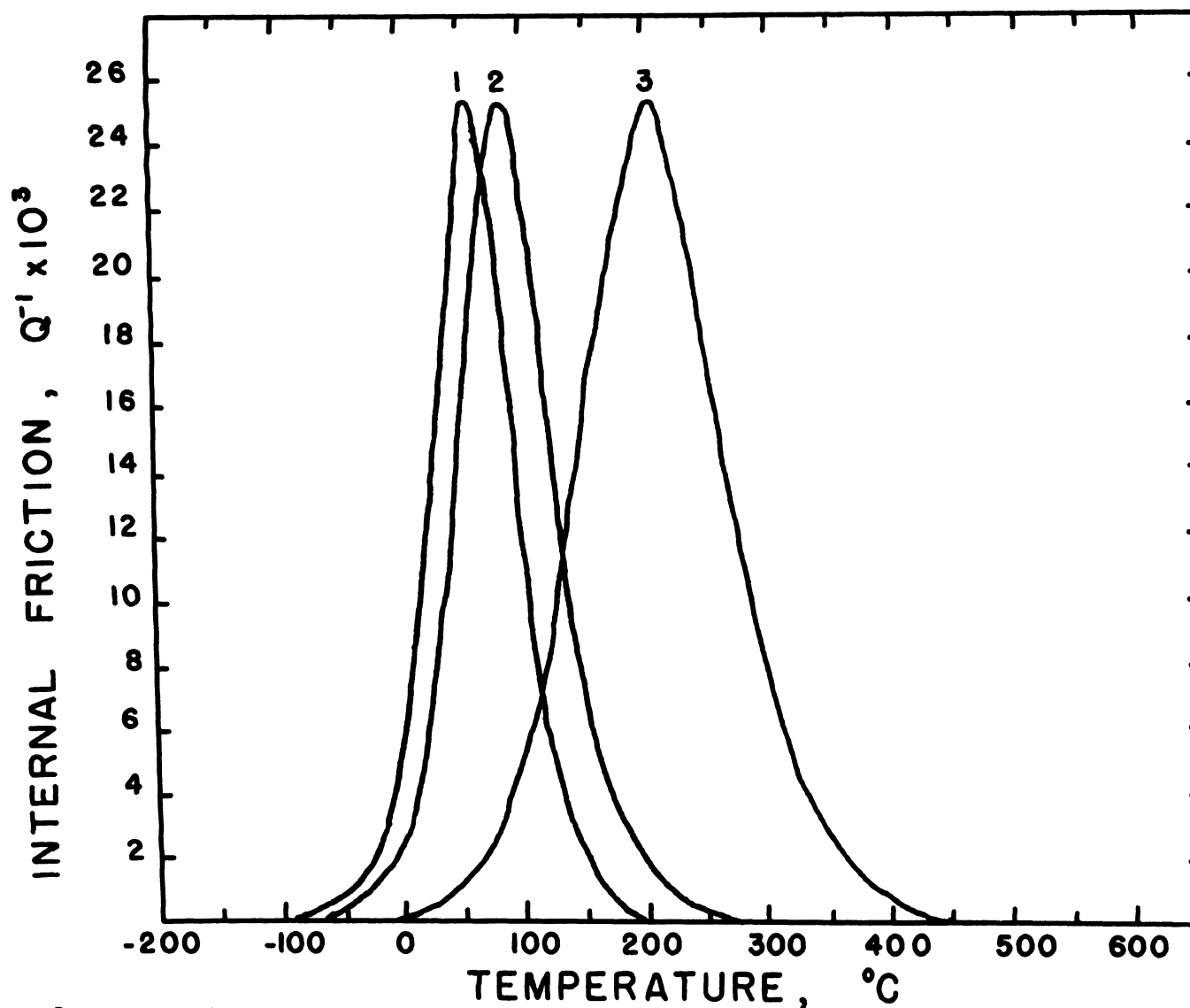


Figure 8. Comparison of Internal Friction Data on Torsion Pendulum and Sonic Damping Equipment, $0.5\text{Li}_2\text{O} \cdot 0.5\text{Na}_2\text{O} \cdot \text{Al}_2\text{O}_3 \cdot 2.0\text{SiO}_2$ Glass, Frequency (1) 0.0914 Hz., (2) 1.044 Hz., (3) 2751 Hz.

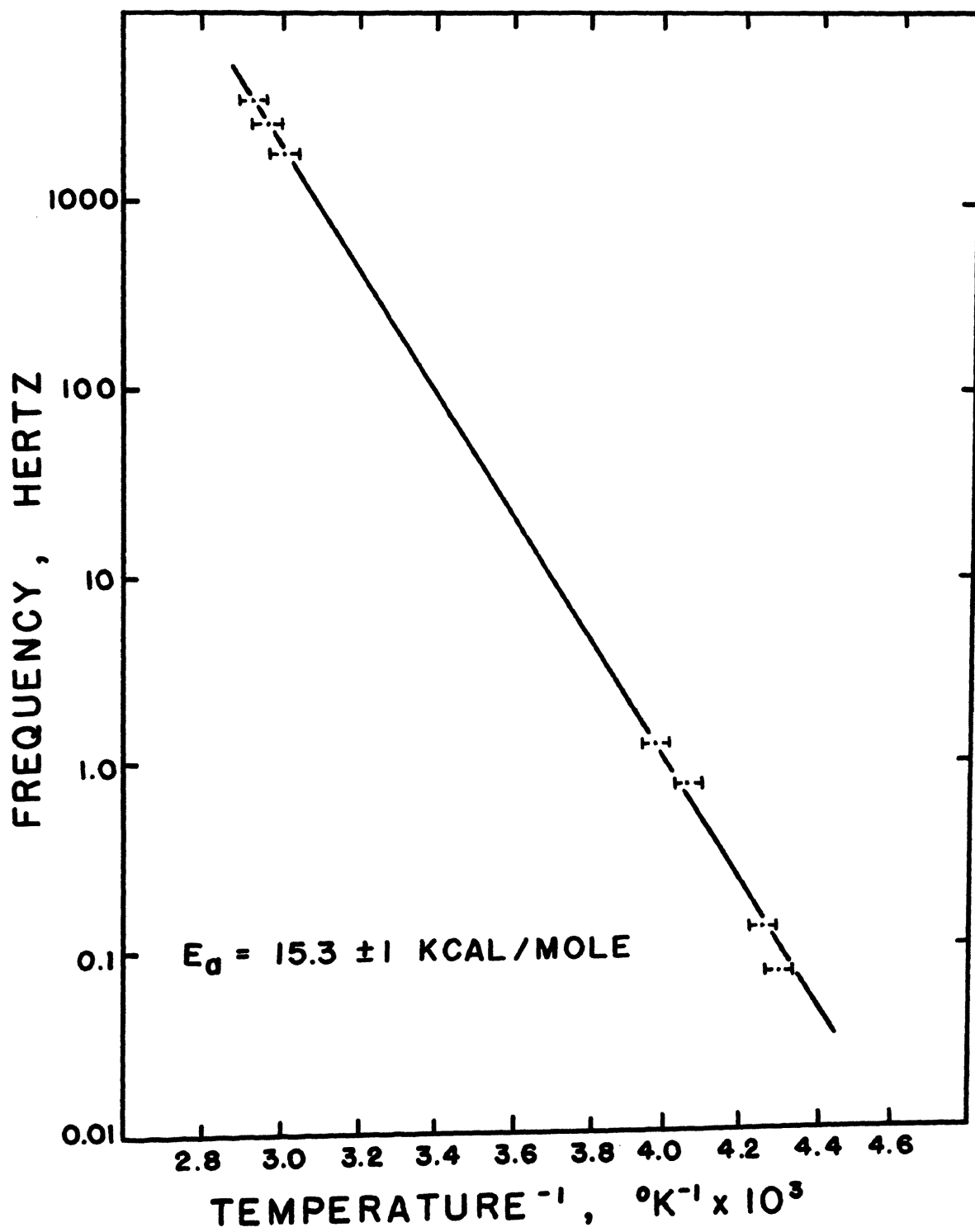


Figure 9. Activation Energy, $\text{Li}_2\text{O} \cdot \text{Al}_2\text{O}_3 \cdot 2.0\text{SiO}_2$ Glass.

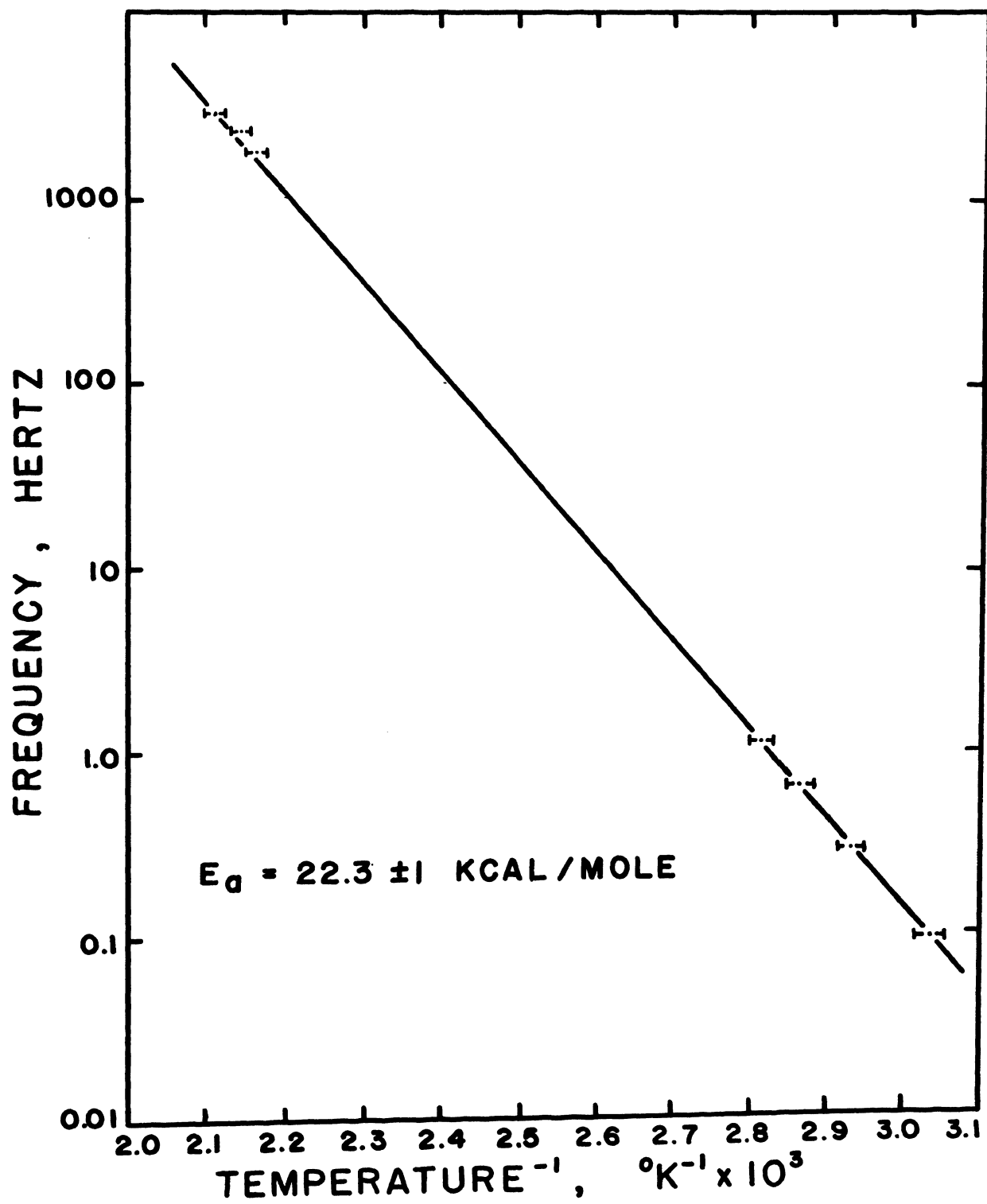


Figure 10. Activation Energy, $0.5\text{Li}_2\text{O} \cdot 0.5\text{Na}_2\text{O} \cdot \text{Al}_2\text{O}_3 \cdot 2.0\text{SiO}_2$ Glass.

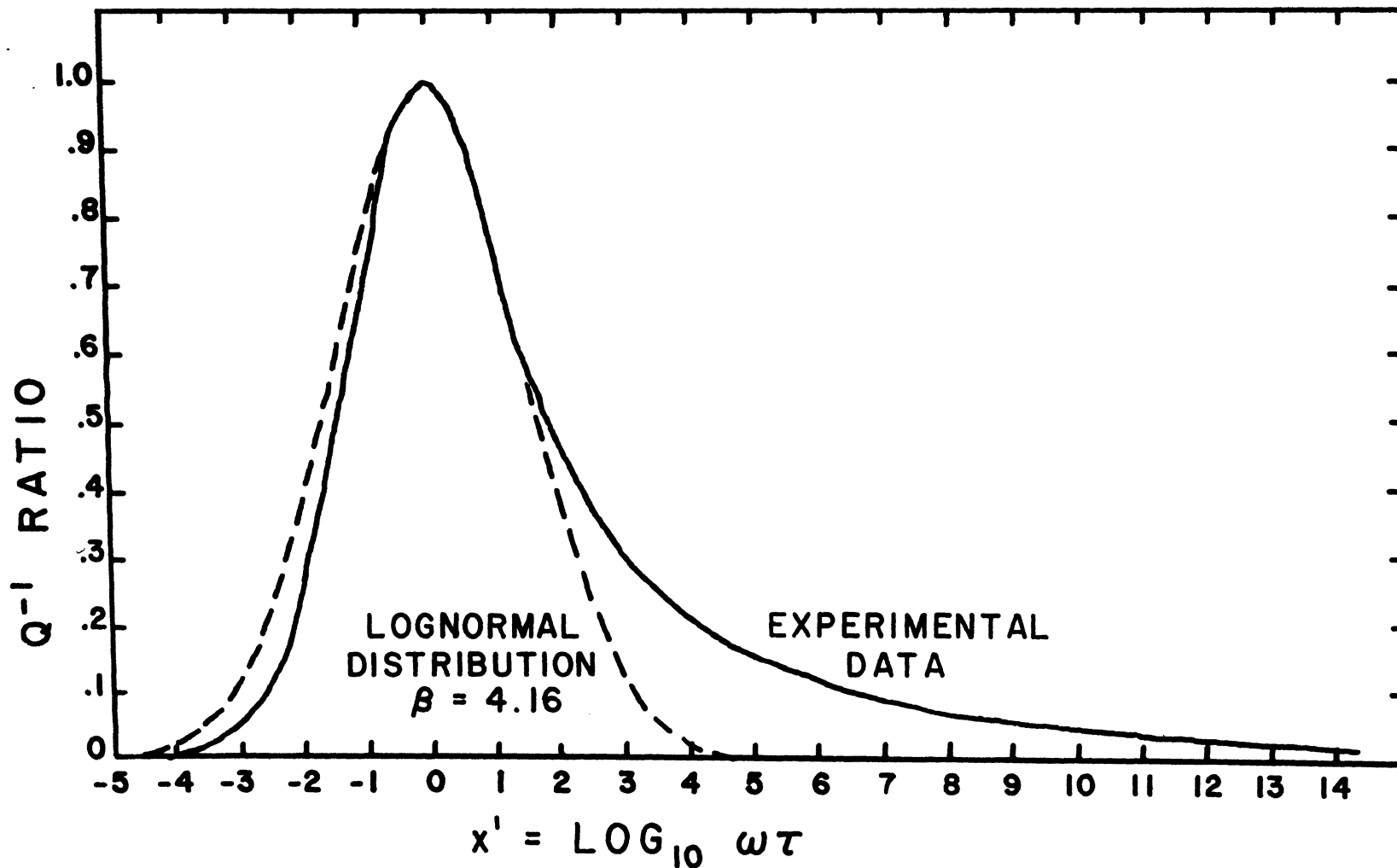


Figure 11. Comparison of Internal Friction Experimental Data and Analytical Solution, $\text{Li}_2\text{O} \cdot \text{Al}_2\text{O}_3 \cdot 2.0\text{SiO}_2$ Glass, Frequency 0.76 HZ.

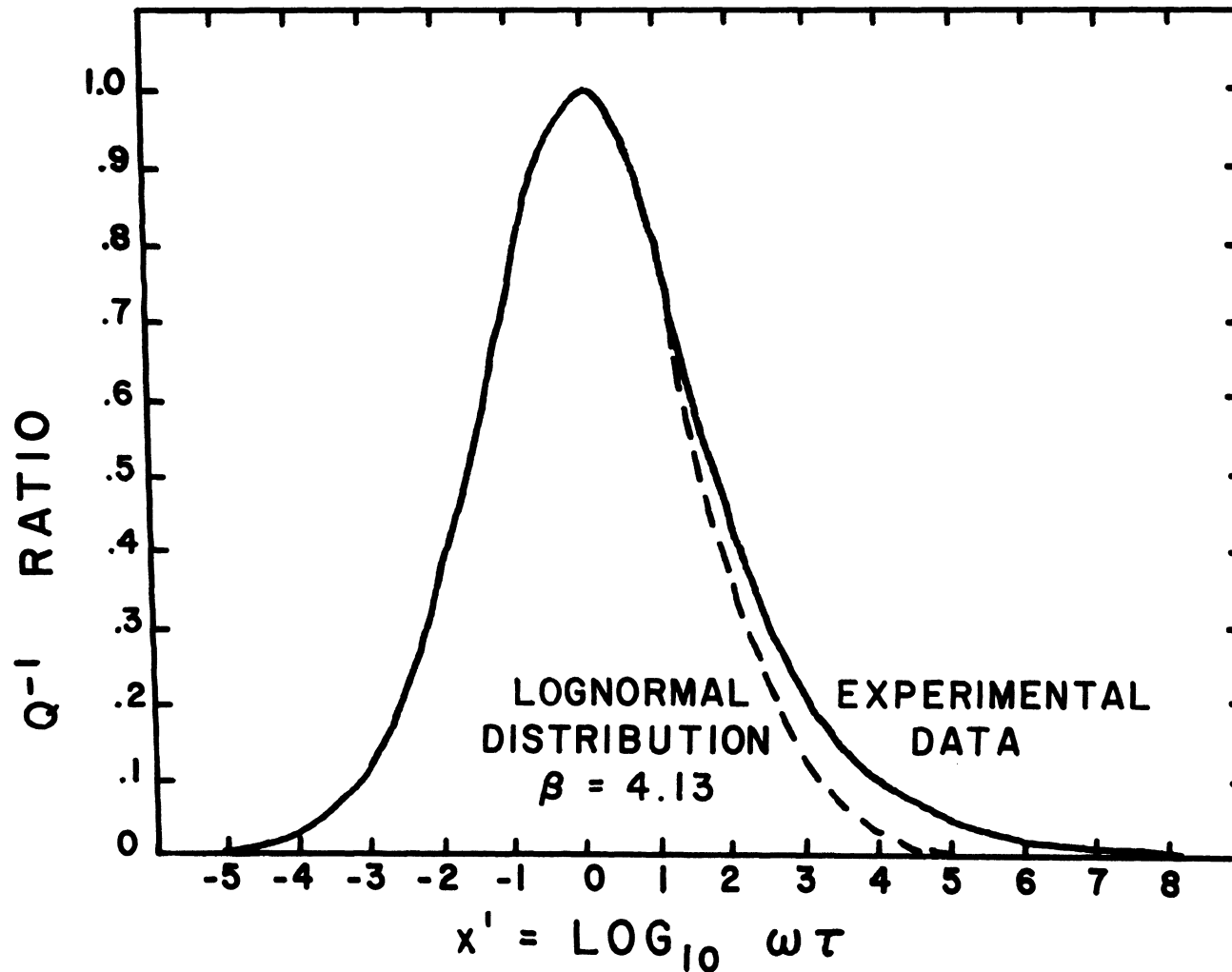


Figure 12. Comparison of Internal Friction Experimental Data and Analytical Solution, $0.5\text{Li}_2\text{O} \cdot 0.5\text{Na}_2\text{O} \cdot \text{Al}_2\text{O}_3 \cdot 2.0\text{SiO}_2$ Glass, Frequency 0.644 HZ.

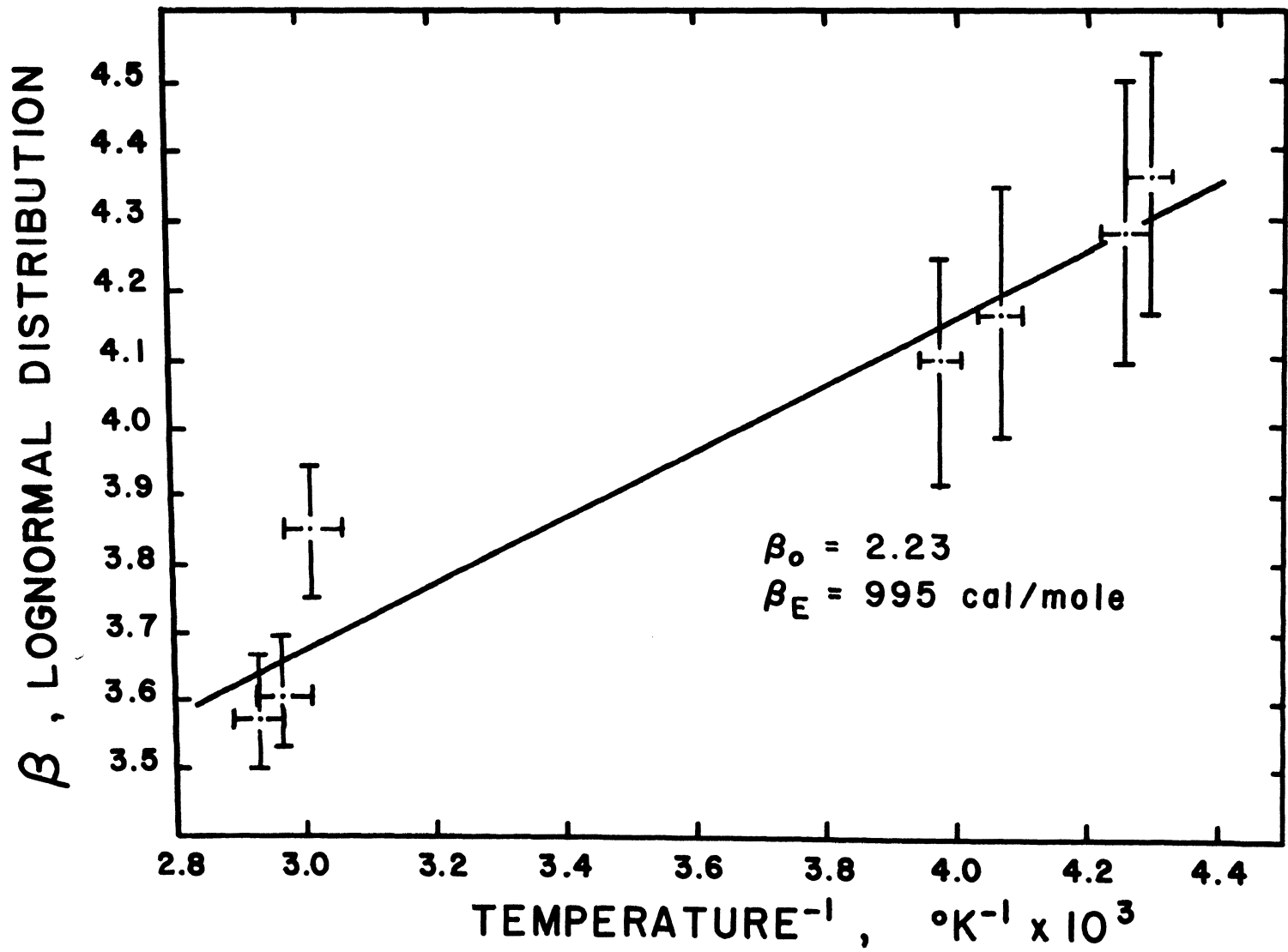


Figure 13. β Variation with Temperature, $\text{Li}_2\text{O} \cdot \text{Al}_2\text{O}_3 \cdot 2.0\text{SiO}_2$ Glass.

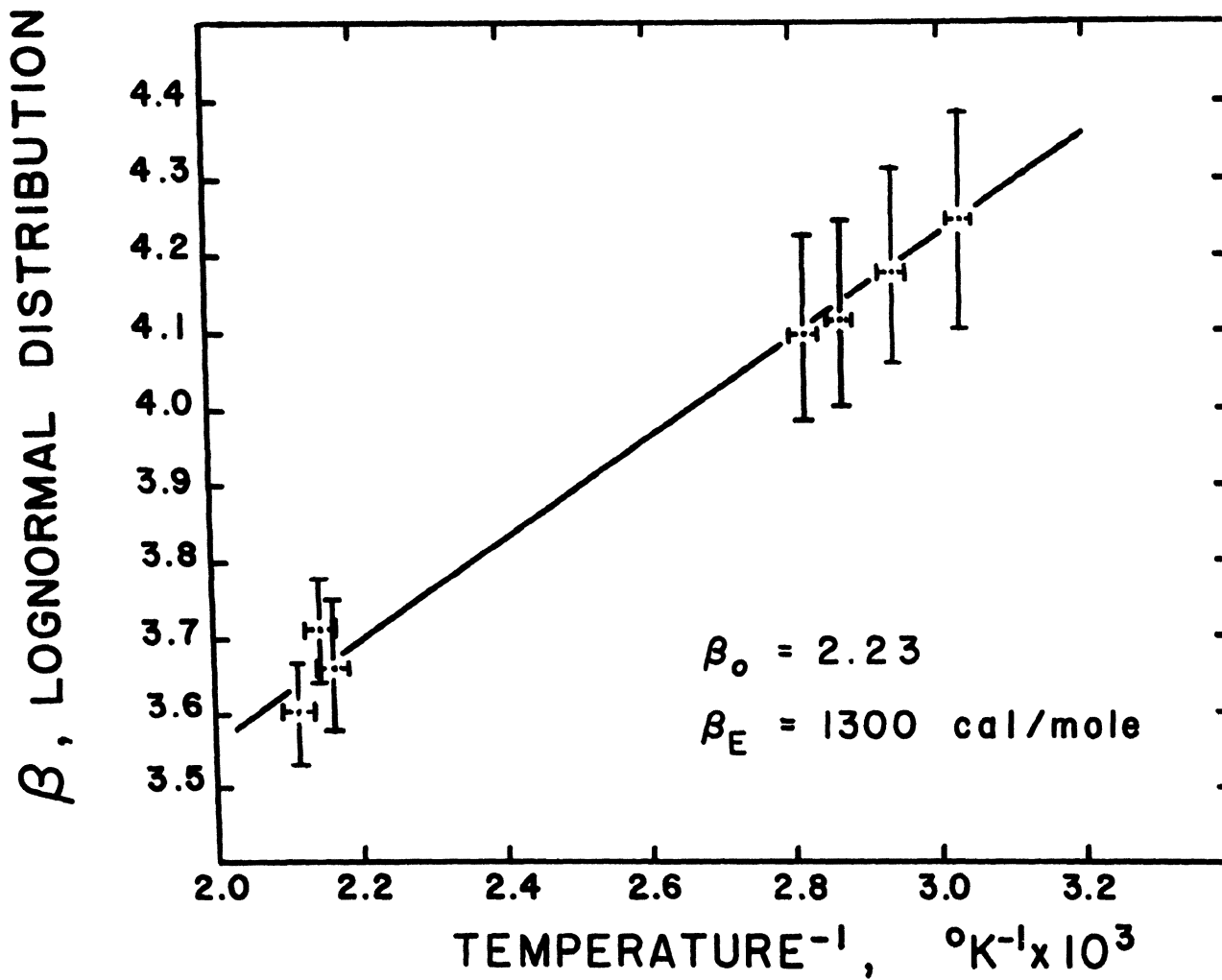


Figure 14. β Variation with Temperature, $0.5\text{Li}_2\text{O} \cdot 0.5\text{Na}_2\text{O} \cdot \text{Al}_2\text{O}_3 \cdot 2.0\text{SiO}_2$ Glass.

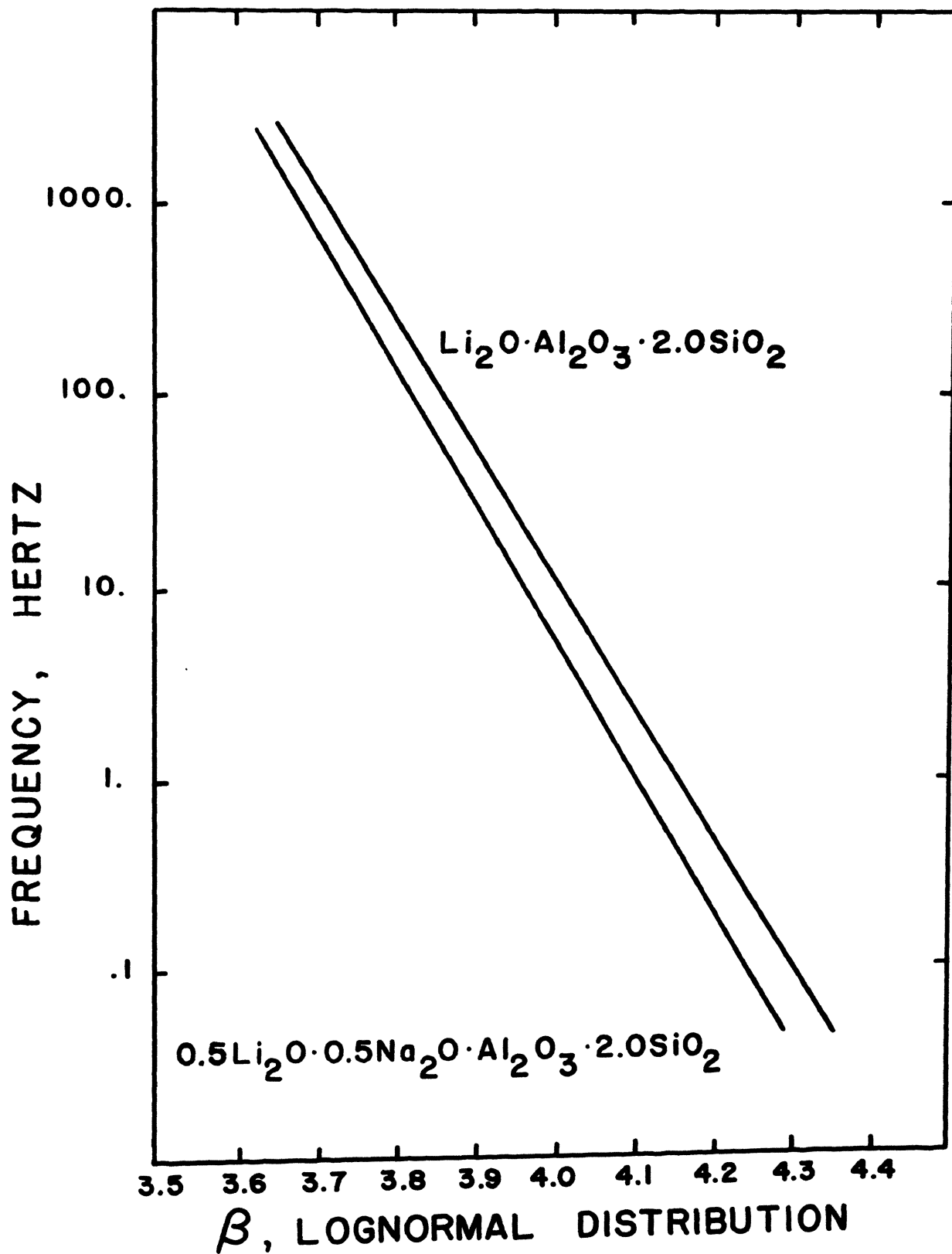


Figure 15. β Variation with Frequency.

TABLE I

Operating Limits of Experimental Equipment

	FREQUENCY RANGE (HERTZ)	TEMPERATURE RANGE (°C)	TEMPERATURE GRADIENT	HEATING RATE (°C/min)	ACCURACY OF INTERNAL FRICTION	PEAK TEMPERATURE REPRODUCIBILITY (°C)
SONIC DAMPING EQUIPMENT	800 to 10,000	-140 to 650	4°C over 6 in. zone	1.0 to 1.5	±2%	±5
TORSION PENDULUM	0.07 to 1.25	-180 to 650	3°C	1.0 to 1.5	±2%	±2

TABLE II

Internal Friction Data, $\text{Li}_2\text{O}\cdot\text{Al}_2\text{O}_3\cdot 2.0\text{SiO}_2$ Glass

FREQUENCY (HERTZ)	PEAK HEIGHT ABOVE BACKGROUND (10^{-3}) $\pm 0.2 \times 10^{-3}$	PEAK TEMPERATURE ($^{\circ}\text{C}$)	HALF-HEIGHT PEAK WIDTH $\delta(T^{-1})$ ($10^{-3} \text{ } ^{\circ}\text{K}^{-1}$)	β LOGNORMAL DISTRIBUTION
3293.	10.1	68 ± 5	$0.890 \pm .020$	$3.57 \pm .09$
2571.	9.6	64 ± 5	$0.895 \pm .020$	$3.60 \pm .09$
1933.	9.6	58 ± 5	$0.943 \pm .020$	$3.85 \pm .10$
1.20	10.1	-22 ± 2	$0.986 \pm .033$	$4.10 \pm .17$
.76	10.3	-27 ± 2	$1.000 \pm .035$	$4.16 \pm .18$
.136	10.2	-38 ± 2	$1.023 \pm .038$	$4.28 \pm .20$
.0734	10.2	-40 ± 2	$1.035 \pm .039$	$4.36 \pm .20$

TABLE III

Internal Friction Data, $0.5\text{Li}_2\text{O}\cdot 0.5\text{Na}_2\text{O}\cdot \text{Al}_2\text{O}_3\cdot 2.0\text{SiO}_2$ Glass

FREQUENCY (HERTZ)	PEAK HEIGHT ABOVE BACKGROUND (10^{-3}) $\pm 0.5 \times 10^{-3}$	PEAK TEMPERATURE ($^{\circ}\text{C}$)	HALF-HEIGHT PEAK WIDTH $\delta(T-1)$ ($10^{-3} \text{ } ^{\circ}\text{K}^{-1}$)	β LOGNORMAL DISTRIBUTION
2751.	25.2	200 ± 5	$0.613 \pm .010$	$3.60 \pm .07$
2024.	24.6	193 ± 5	$0.628 \pm .010$	$3.71 \pm .07$
1756.	24.8	189 ± 5	$0.621 \pm .010$	$3.66 \pm .09$
1.044	25.1	82 ± 2	$0.679 \pm .016$	$4.10 \pm .11$
.644	25.1	76 ± 2	$0.681 \pm .017$	$4.13 \pm .12$
.296	25.2	68 ± 2	$0.689 \pm .018$	$4.18 \pm .12$
.0914	25.1	57 ± 2	$0.696 \pm .019$	$4.25 \pm .14$

TABLE IV

Comparison of Internal Friction Data Before and After
48 Hour Heat Treatment

	PEAK TEMPERATURE (°C)	PEAK HEIGHT ABOVE BACKGROUND (10 ⁻³)	PEAK FREQUENCY (HERTZ)	β PARAMETER
NORMAL MEASUREMENT	58.5	9.6	1933	3.85
48 HOUR HEAT TREATMENT AT 425°C	56.5	9.3	1935	3.75

TABLE V

Distributions in Activation Entropy

GLASS	β_0	ACTIVATION ENTROPY EQUATION (1) (CAL/MOLE ⁰ K)	SPREAD OF ACTIVATION ENTROPY VALUES 95% OF DISTRIBUTION (CAL/MOLE ⁰ K)	RANGE OF ACTIVATION ENTROPY VALUES (CAL/MOLE ⁰ K)
Li ₂ O·Al ₂ O ₃ · 2.0SiO ₂	2.23 (Figure 13)	6.7	±3.1	3.6 to 9.8
0.5Li ₂ O·0.5Na ₂ O· Al ₂ O ₃ ·2.0SiO ₂	2.23 (Figure 14)	7.7	±3.1	4.6 to 10.8

VI. APPENDICES

APPENDIX A

Chemical Analysis of Raw Materials

Li_2CO_3 used in $\text{Li}_2\text{O}\cdot\text{Al}_2\text{O}_3\cdot 2.0\text{SiO}_2$ Glass

United Mineral & Chemical Corp. Analysis Report 4/17/68

Element	Concentration Parts Per Million (PPM)
Aluminum	<1
Calcium	3
Iron	3
Lead	<1
Magnesium	<1
Sodium	2

Al_2O_3 used in $\text{Li}_2\text{O}\cdot\text{Al}_2\text{O}_3\cdot 2.0\text{SiO}_2$ Glass

United Mineral & Chemical Corp. Analysis Report 5/28/68

Element	Concentration (PPM)
Calcium	<1
Copper	<1
Iron	1
Magnesium	1
Silicon	2
Sodium	<1

APPENDIX A (continued)

Li_2CO_3 used in $0.5\text{Li}_2\text{O}\cdot 0.5\text{Na}_2\text{O}\cdot \text{Al}_2\text{O}_3\cdot 2.05\text{SiO}_2$ Glass

Fisher Scientific Company, Lot Analysis 780043

Item	Concentration Percent
Chloride	0.001
Calcium	0.007
Heavy Metals (as Lead)	0.0004
Iron	0.0007
Insoluble in Dilute Hcl	0.02
Nitrate (NO_3)	0.0003
Ammonium (NH_4)	0.0002
Sulfur compounds (as SO_4)	0.04
Potassium	0.02
Sodium	0.07

Al_2O_3 used in $0.5\text{Li}_2\text{O}\cdot 0.5\text{Na}_2\text{O}\cdot \text{Al}_2\text{O}_3\cdot 2.0\text{SiO}_2$ Glass

Fisher Scientific Company, Lot Analysis 766491

Item	Concentration Percent
Chloride	0.001
Iron	0.001
Heavy Metals (as Lead)	0.0005
Sulfate (SO_4)	0.007
Silicate	0.02
Alkalies and Earths	0.36

APPENDIX A (continued)

Na_2CO_3 used in $0.5\text{Li}_2\text{O}\cdot 0.5\text{Na}_2\text{O}\cdot \text{Al}_2\text{O}_3\cdot 2.0\text{SiO}_2$ Glass

Fisher Scientific Company, Lot Analysis 785405

Item	Concentration Percent
Iron	0.0001
Silica	0.003
Chloride	0.0004
Arsenic	0.00003
Insoluble matter	0.008
Nitrogen Compounds	0.0008
Phosphate (PO_4)	0.0003
Sulfur Compounds (as SO_4)	0.003
Ammonium Hydroxide	0.006
Calcium and Magnesium	0.004
Potassium	0.001
Heavy Metals (as Lead)	0.0001

APPENDIX B

Peak Height Determination and Correction

An internal friction peak with a single relaxation time should have a peak height given by the equation

$$Q^{-1} = \frac{\Delta}{2} \quad (9)$$

$$Q^{-1} = \text{Internal friction}$$

$$\Delta = \text{Relaxation ratio}$$

Equation (9) is obtained from the equation

$$Q^{-1} = \Delta \frac{\omega \tau}{1 + \omega^2 \tau^2} \quad (10)$$

by noting that at the peak $\omega \tau = 1$. If the internal friction peak in a material contains a distribution of relaxation times, the result is a shorter and wider peak. However, the peak containing the distribution of relaxation times has the same area as a peak with a single relaxation time. Copley and Oakley⁽²⁹⁾ reported that the areas under the curves they obtained remained essentially constant. They used as a measure of the area the net peak height times the peak width at half-height. In Tables II and III, the net peak height and the width at half-height, ($\delta (1/T)$), are reported. If these two are multiplied together a measure of the area is obtained. From these tables it appears that at the high frequencies the area is decreasing. This is not the case as will be explained.

APPENDIX B (continued)

A point not so obvious is that the peak height is proportional to Δ , the relaxation ratio (see Equations (5), (7), (9), and (10)), and the relaxation ratio is not constant for measurements on the torsion pendulum and the sonic damping equipment. The relaxation ratio, Δ , is determined from the equation

$$\Delta = \frac{M_U - M_R}{M_R} \quad (11)$$

M_U = Unrelaxed Modulus (low temperature)

M_R = Relaxed Modulus (high temperature)

On the torsion pendulum the appropriate modulus is the shear modulus, relating to torsion, while on the sonic damping equipment, Young's modulus is applicable, relating to flexure.

Zener⁽⁴²⁾ has obtained the following equation

$$\Delta_G = 3 \frac{G_U}{E_U} \Delta_E \quad (12)$$

Δ_G = Relaxation ratio obtained in shear

G_U = Unrelaxed shear modulus

E_U = Unrelaxed Young's modulus

Δ_E = Relaxation ratio obtained in flexure

In isotropic materials the shear modulus and Young's modulus are related by the equation

$$G = \frac{E}{2(1+\nu)} \quad (13)$$

APPENDIX B (continued)

ν = Poisson's ratio

Substituting (13) into (12) gives

$$\Delta_G = \frac{3}{2(1+\nu)} \Delta_E \quad (14)$$

For a normal value of Poisson's ratio, 0.3, it can be seen that the relaxation ratio, Δ , should be approximately 15 percent larger when obtained from a test in torsion than from flexure. The data presented in Table VI and VII show this to be true. On the single alkali glass the relaxation ratios obtained on the torsion pendulum averaged 12.5 percent larger than those obtained on the sonic damping equipment. For the mixed alkali glass it was 15 percent. Thus, if nothing were changed except measuring a specimen on the two pieces of equipment, one would expect the internal friction peak height to be approximately 15 percent larger on the torsion pendulum.

There is another factor affecting the peak height, however. As the distribution of relaxation times gets wider (broader) the peak should become smaller. It has been shown that β varies with temperature. As the peak occurred at a higher temperature the peak became narrower meaning it should have increased in height. In Tables II and III it is seen that the peak height obtained is relatively constant. The two factors, different relaxation ratios and peak broadening have each essentially cancelled out the effect of

APPENDIX B (continued)

the other. Also in Tables VI and VII are the net peak heights obtained from the experimental data and the corrected peak heights to compensate for the different relaxation ratios. When the appropriate factors are multiplied to get a measure of the area the numbers are constant within experimental accuracy.

Rather than multiply two factors together to get a measure of the area a planimeter was used to measure the enclosed area of all the curves. In this case the area of all measurements on the single alkali glass was within ± 0.04 of the average and the same variation was found in area on the mixed alkali glass.

Comparing the peak heights obtained on both pieces of equipment isn't correct unless the difference in the relaxation ratio is taken into account. The areas under the curves, based on the corrected peak heights, has remained essentially constant, which is expected.

TABLE VI

Correction of Peak Height for Relaxation Ratio, $\text{Li}_2\text{O}\cdot\text{Al}_2\text{O}_3\cdot 2.0\text{SiO}_2$ Glass

	Δ RELAXATION RATIO	AVERAGE Δ	PERCENT DIFFERENCE	PEAK WIDTH TABLE II 10^{-3} $\delta(1/T)$	PEAK HEIGHT TABLE II 10^{-3}	CORRECTED PEAK HEIGHT	MEASURE OF CORRECTED AREA WIDTH x HEIGHT
SONIC	.061			.890	10.1	11.1	9.9
DAMPING	.055	.058		.895	9.6	10.5	9.5
EQUIPMENT	.057			.943	9.6	10.6	10.0
TORSION	.063			.986	10.1	Same	9.9
	.064		12.5%	1.000	10.3	as	10.3
PENDULUM	.063	.065	Larger	1.023	10.2	Preceding	10.4
	.069			1.035	10.2	Column	10.5

TABLE VII

Correction of Peak Height for Relaxation Ratio, $0.5\text{Li}_2\text{O}\cdot 0.5\text{Na}_2\text{O}\cdot \text{Al}_2\text{O}_3\cdot 2.0\text{SiO}_2$ Glass

	Δ RELAXATION RATIO	AVERAGE Δ	PERCENT DIFFERENCE	PEAK WIDTH TABLE III 10^{-3} $\delta(1/T)$	PEAK HEIGHT TABLE III 10^{-3}	CORRECTED PEAK HEIGHT	MEASURE OF CORRECTED AREA WIDTH x HEIGHT
SONIC	.146			.613	25.2	28.5	17.5
DAMPING	.141	.141		.628	24.6	27.9	17.5
EQUIPMENT	.137			.621	24.8	28.2	17.5
TORSION	.162			.679	25.1	Same	17.0
PENDULUM	.159		15%	.681	25.1	as	17.1
	.158	.162	Larger	.689	25.2	Preceding	17.4
	.169			.696	25.1	Column	17.5

APPENDIX C

Figures of Experimental Data

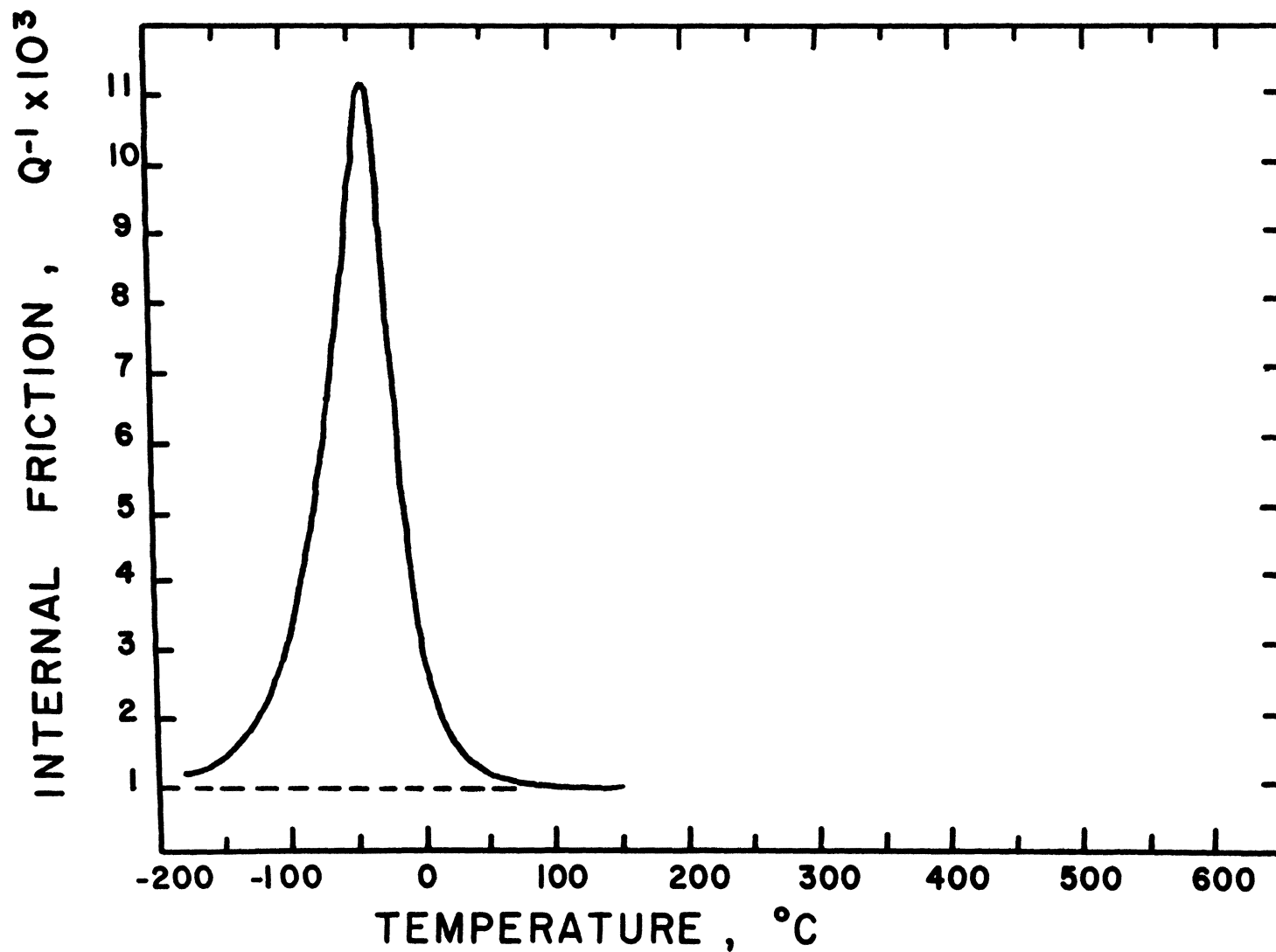


Figure 16. Internal Friction Curve, $\text{Li}_2\text{O} \cdot \text{Al}_2\text{O}_3 \cdot 2.0\text{SiO}_2$ Glass, Frequency 0.0734 HZ.

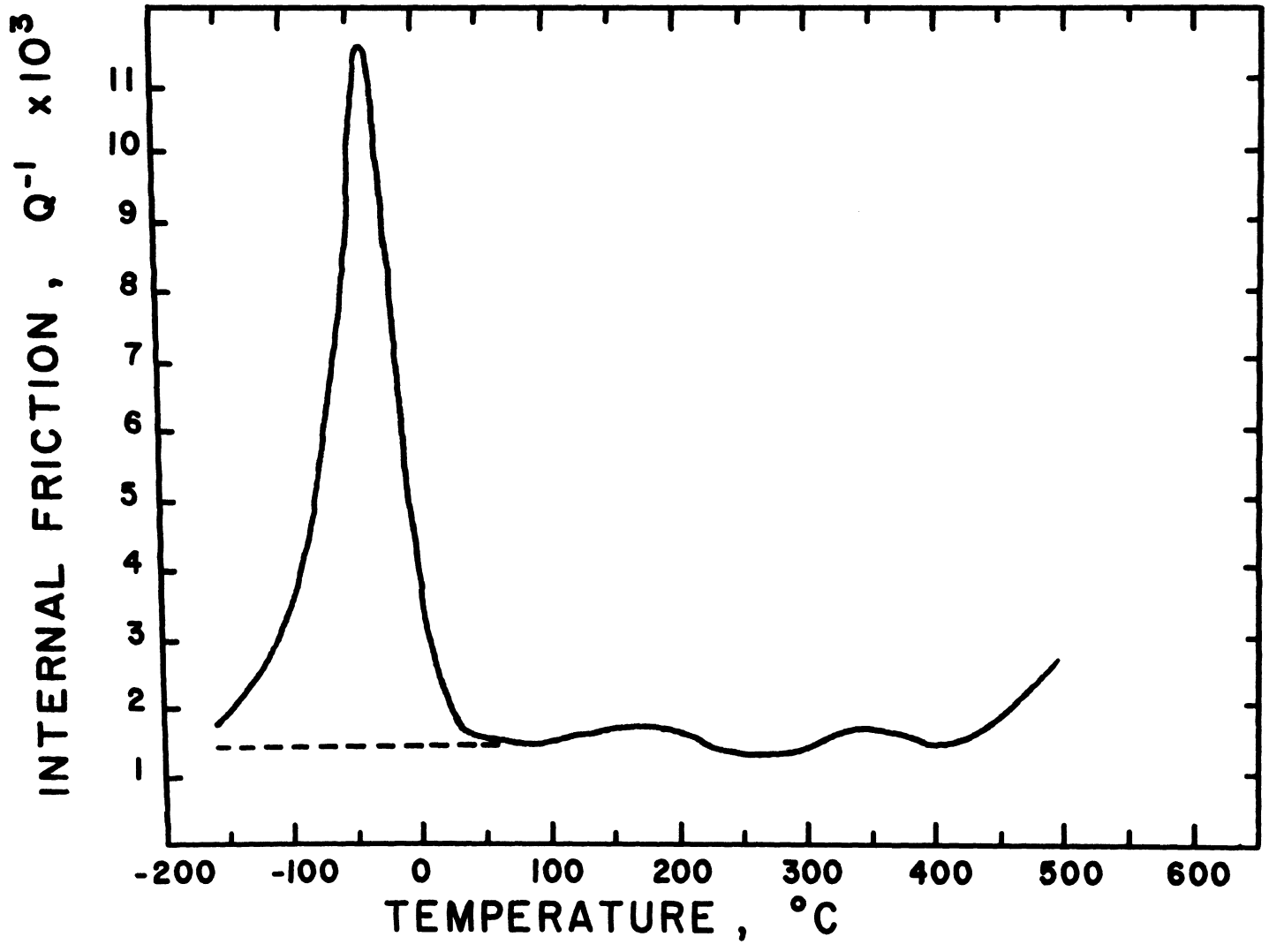


Figure 17. Internal Friction Curve, $\text{Li}_2\text{O} \cdot \text{Al}_2\text{O}_3 \cdot 2.0\text{SiO}_2$ Glass, Frequency 0.136 HZ.

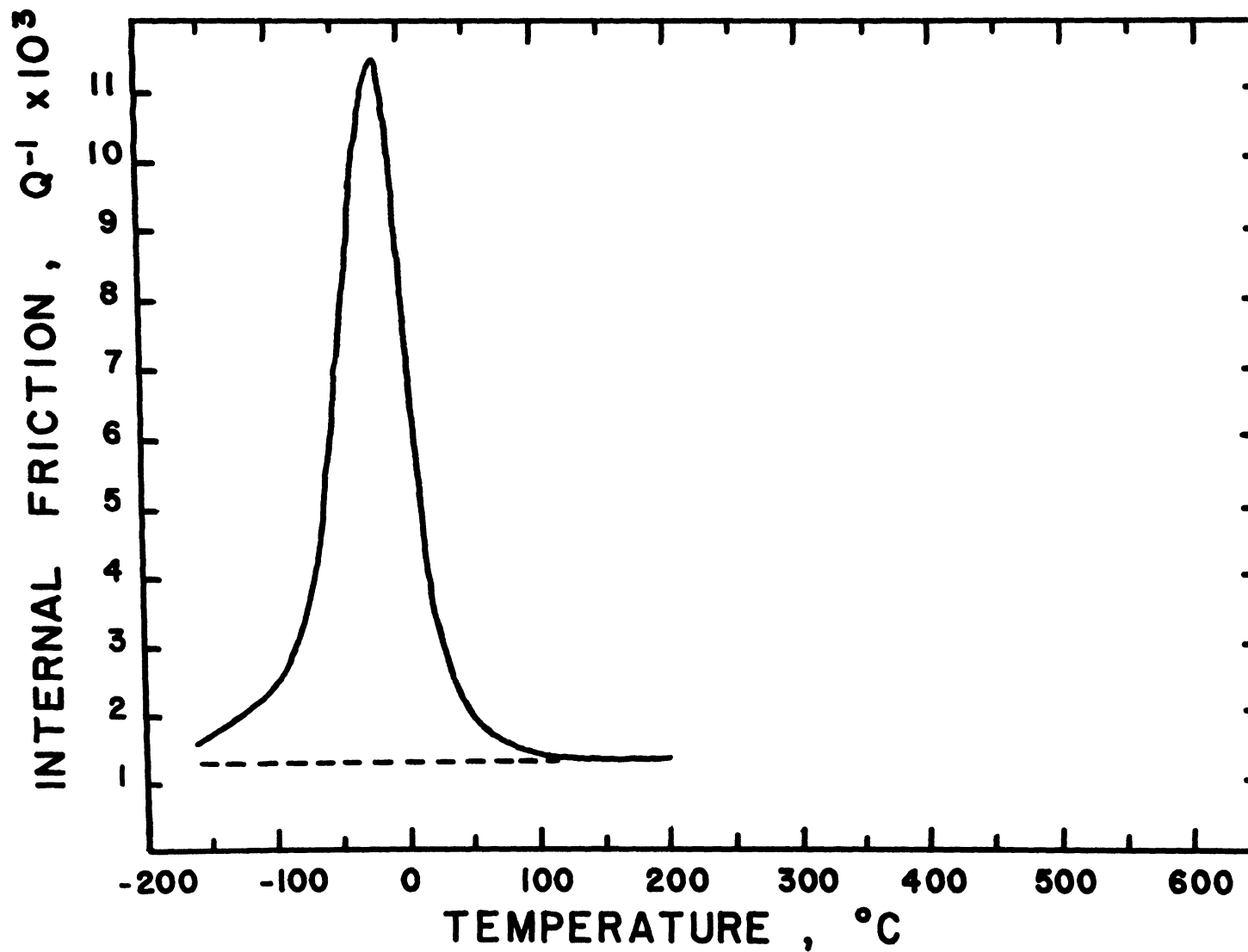


Figure 18. Internal Friction Curve, $\text{Li}_2\text{O}\cdot\text{Al}_2\text{O}_3\cdot 2.0\text{SiO}_2$ Glass, Frequency 1.20 HZ.

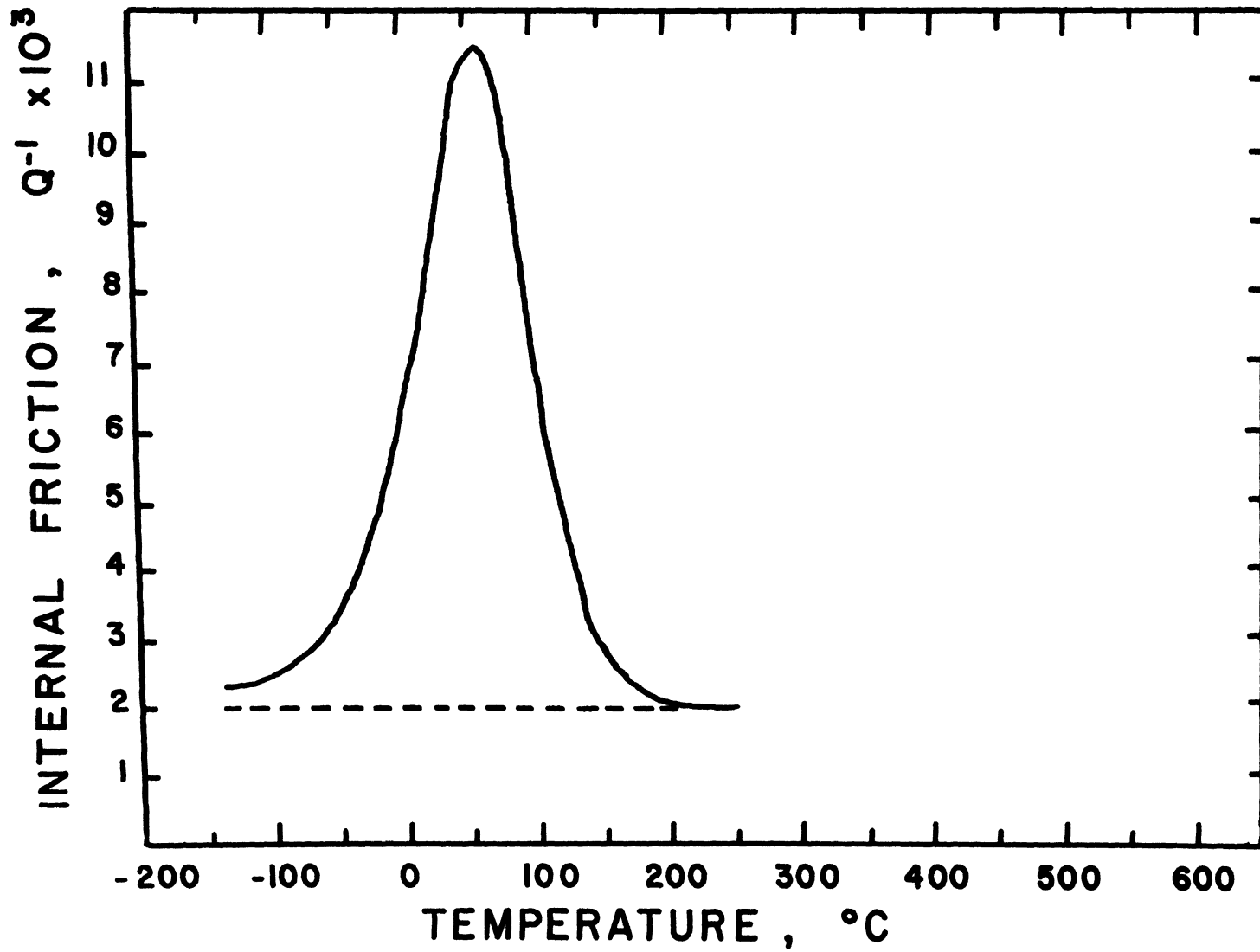


Figure 19. Internal Friction Curve, $\text{Li}_2\text{O}\cdot\text{Al}_2\text{O}_3\cdot 2.0\text{SiO}_2$ Glass, Frequency 1933 HZ.

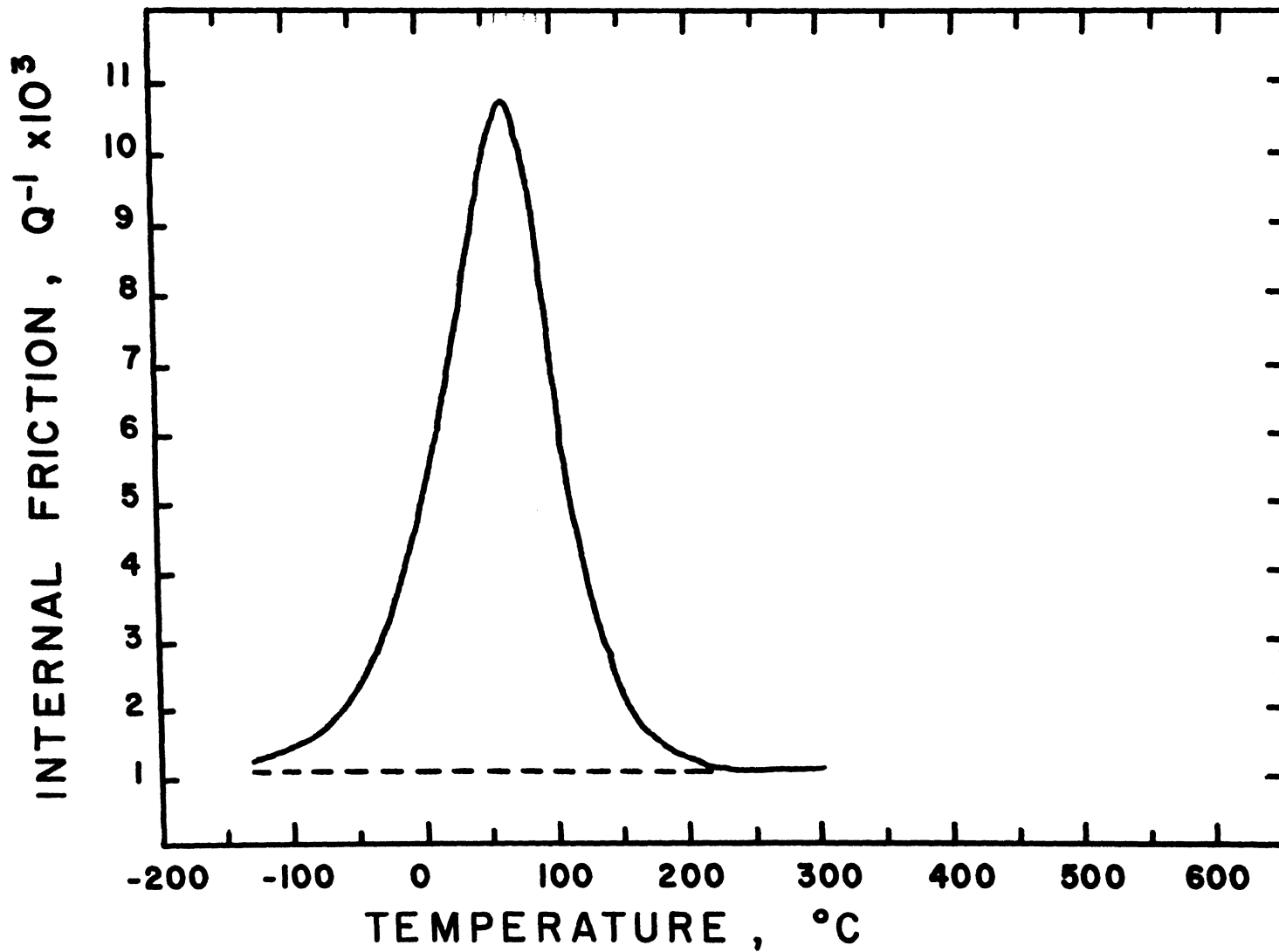


Figure 20. Internal Friction Curve, $\text{Li}_2\text{O}\cdot\text{Al}_2\text{O}_3\cdot 2.0\text{SiO}_2$ Glass, Frequency 2571 HZ.

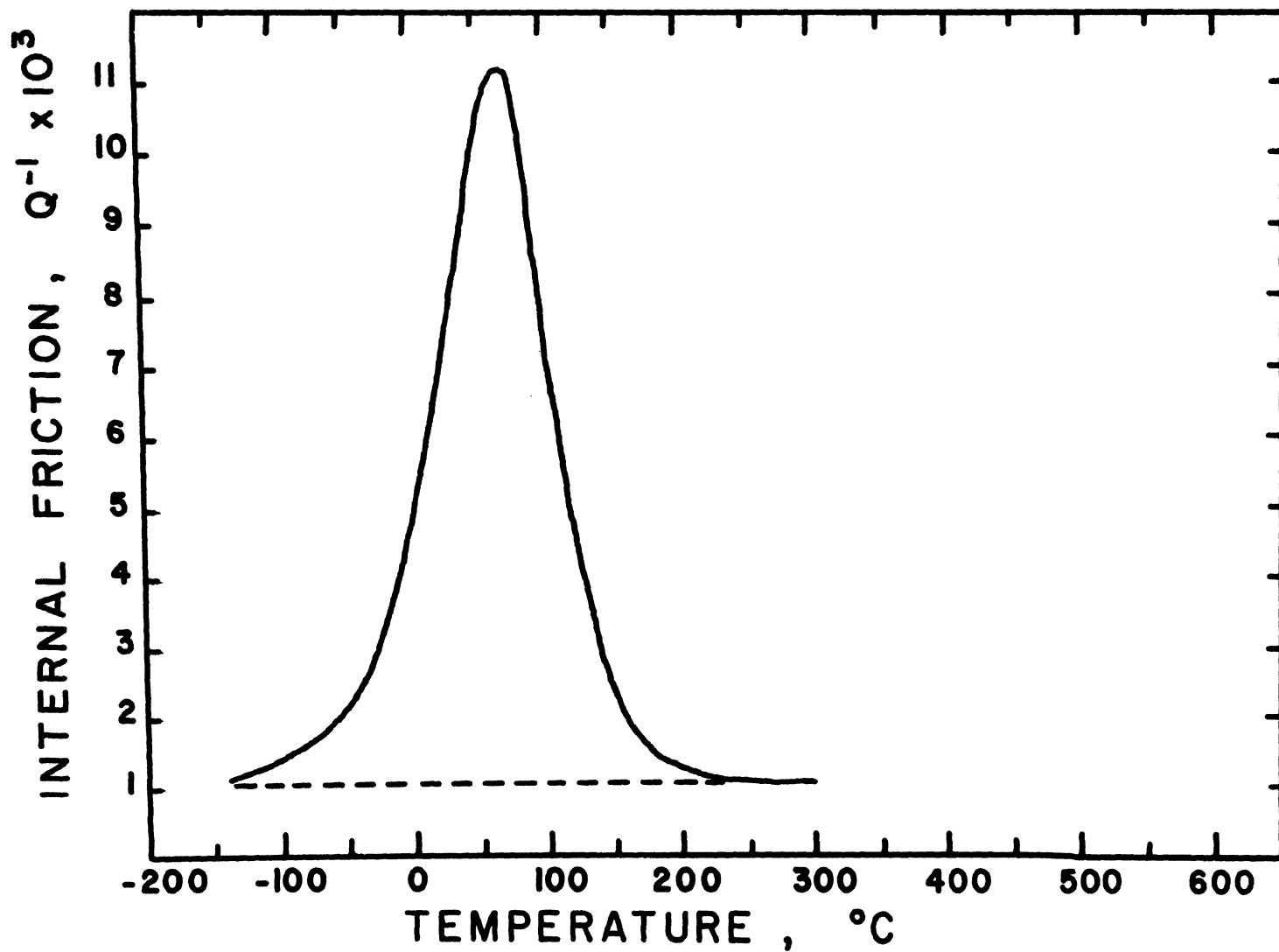


Figure 21. Internal Friction Curve, $\text{Li}_2\text{O} \cdot \text{Al}_2\text{O}_3 \cdot 2.0\text{SiO}_2$ Glass, Frequency 3293 HZ.

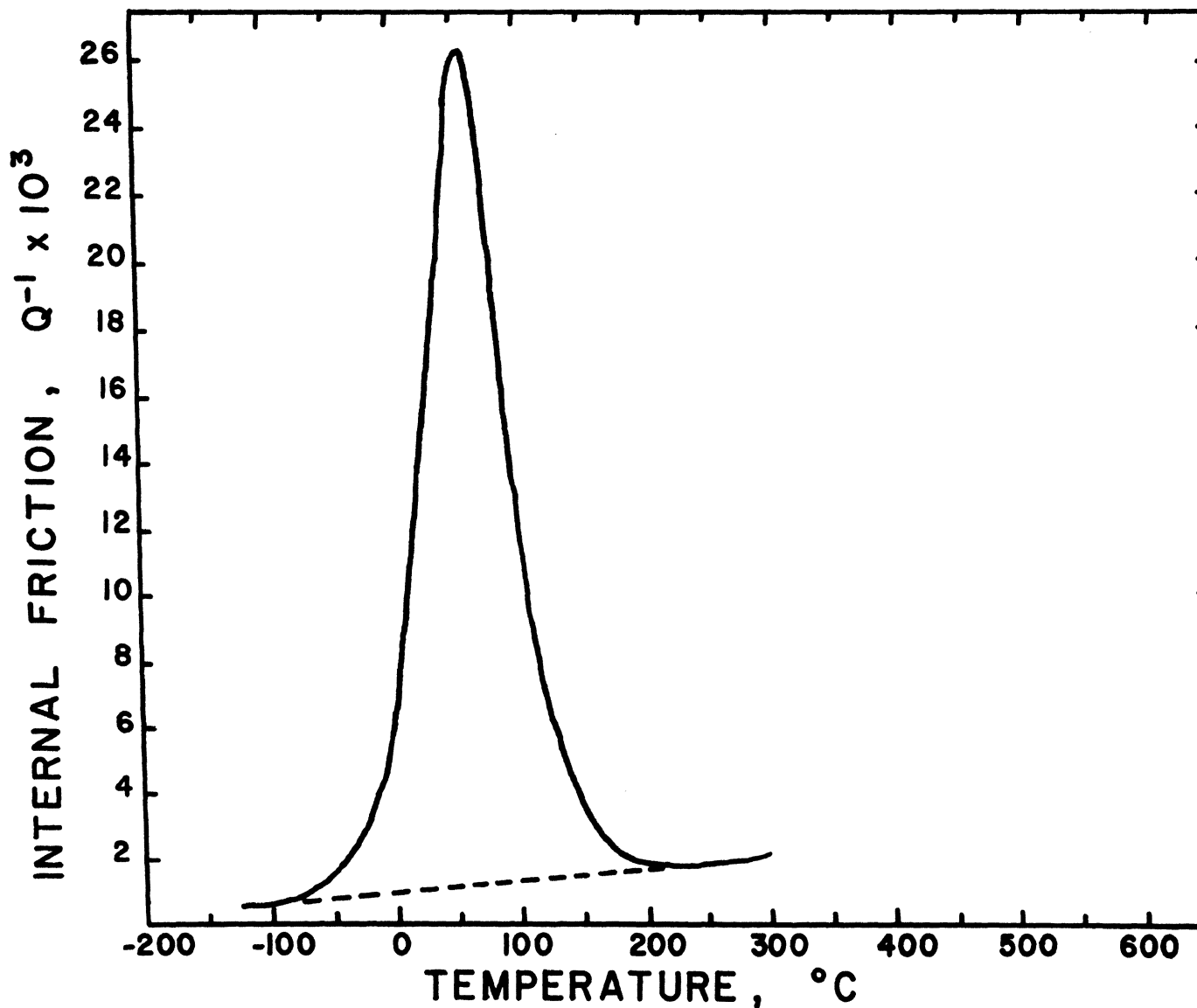


Figure 22. Internal Friction Curve, $0.5Li_2O \cdot 0.5Na_2O \cdot Al_2O_3 \cdot 2.0SiO_2$ Glass, Frequency 0.0914 HZ.

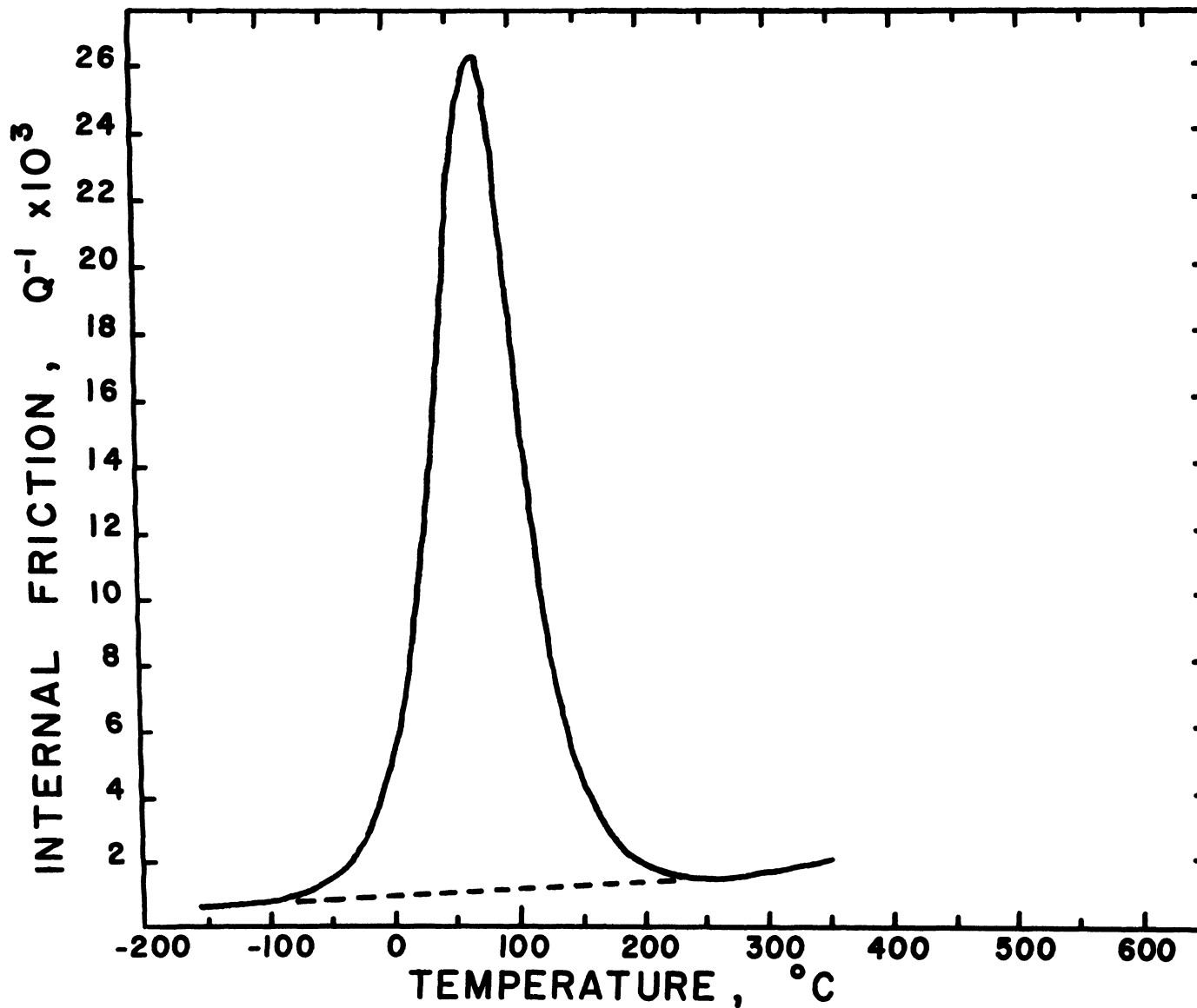


Figure 23. Internal Friction Curve, $0.5\text{Li}_2\text{O}\cdot 0.5\text{Na}_2\text{O}\cdot \text{Al}_2\text{O}_3\cdot 2.0\text{SiO}_2$ Glass, Frequency 0.296 Hz.

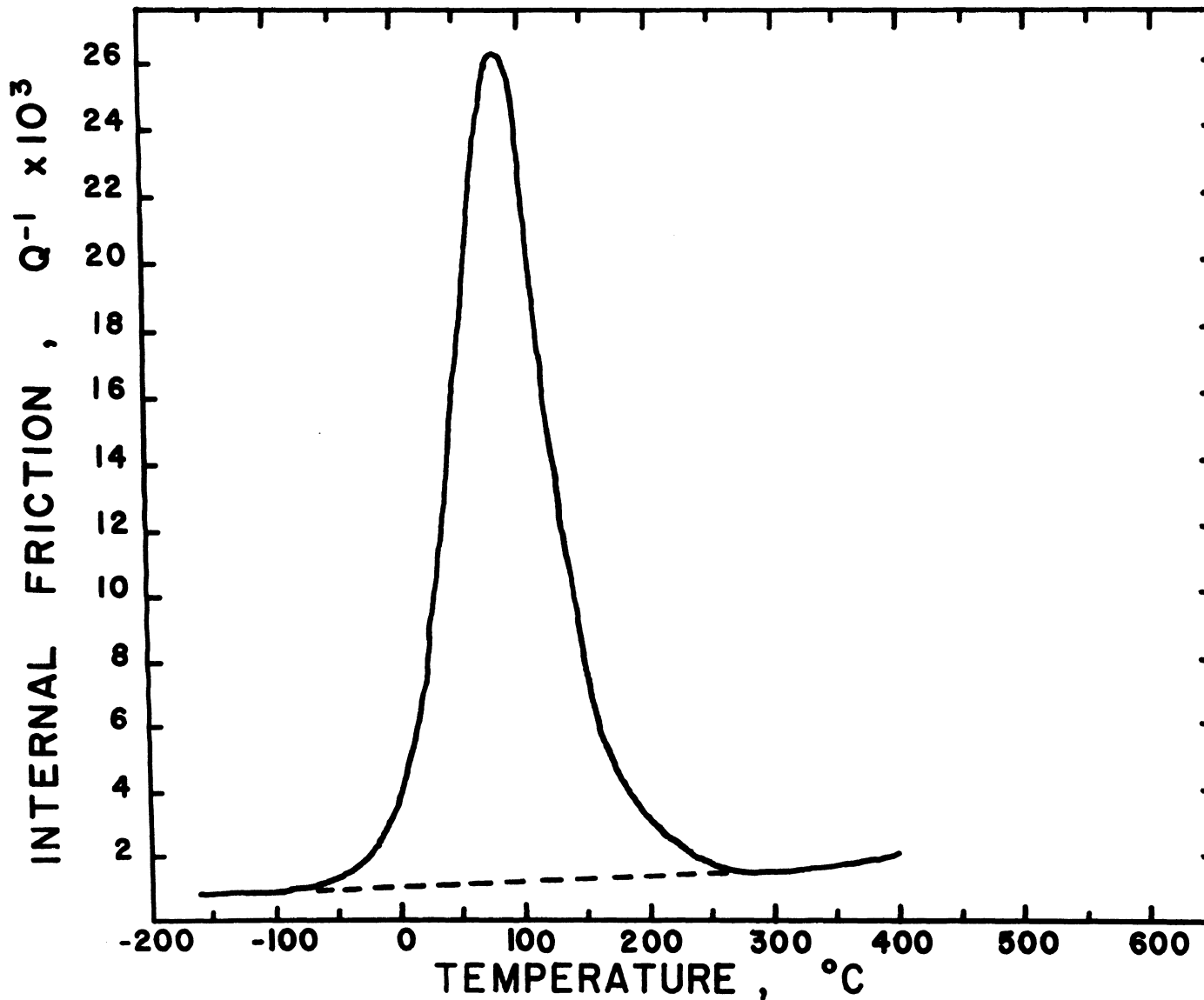


Figure 24. Internal Friction Curve, $0.5\text{Li}_2\text{O}\cdot 0.5\text{Na}_2\text{O}\cdot \text{Al}_2\text{O}_3\cdot 2.0\text{SiO}_2$ Glass, Frequency 1.044 HZ.

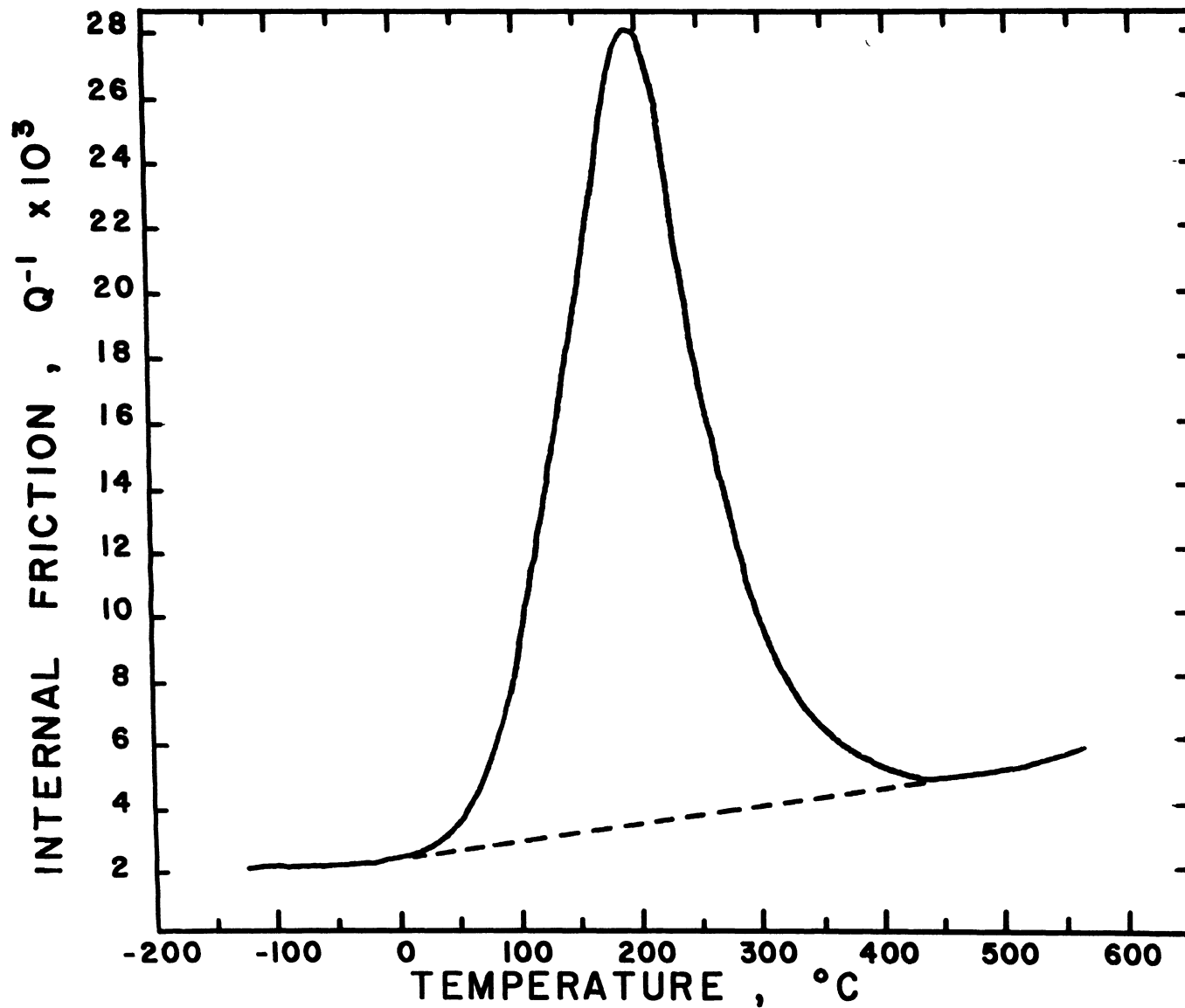


Figure 25. Internal Friction Curve, $0.5\text{Li}_2\text{O} \cdot 0.5\text{Na}_2\text{O} \cdot \text{Al}_2\text{O}_3 \cdot 2.0\text{SiO}_2$ Glass, Frequency 1756 HZ.

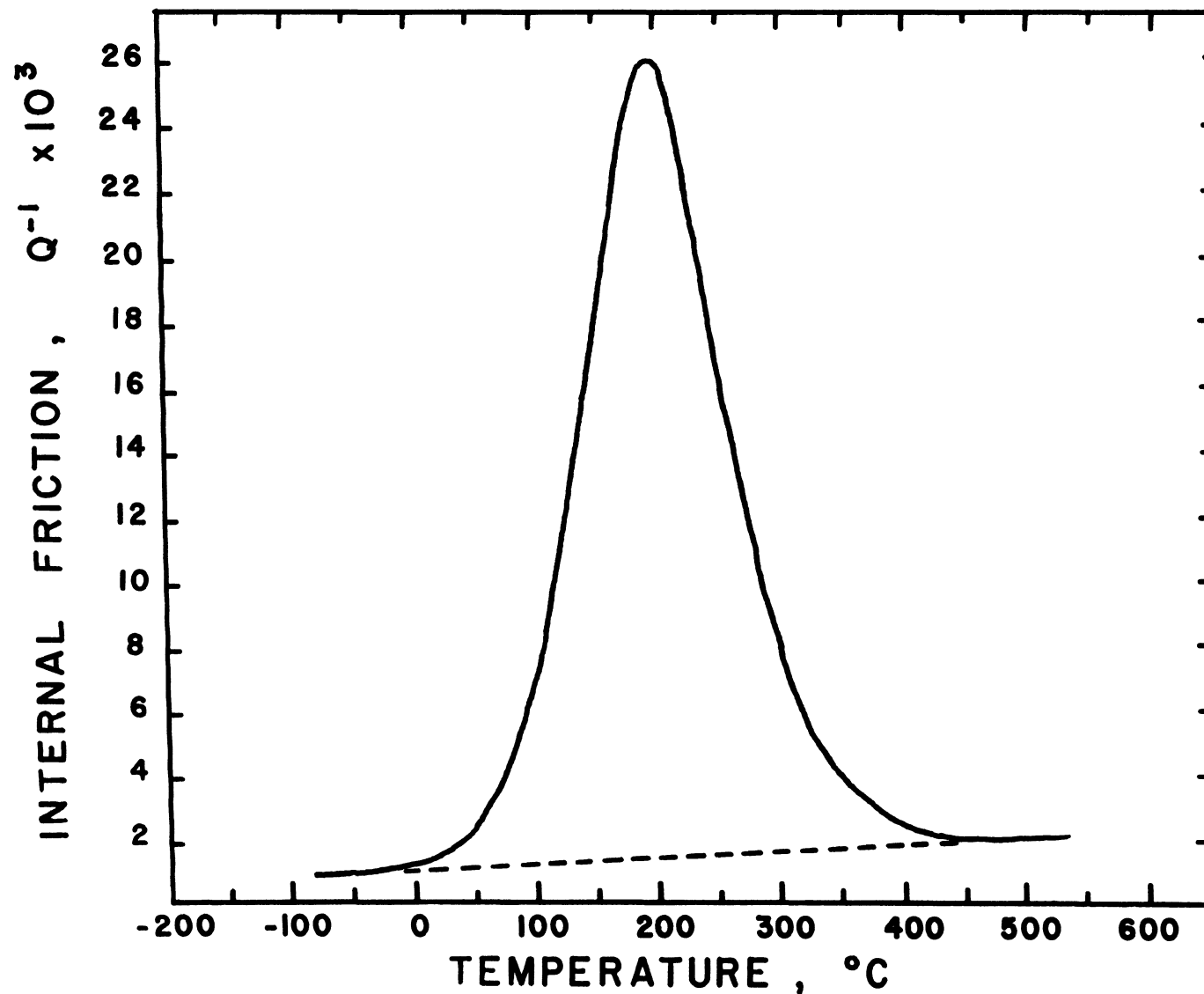


Figure 26. Internal Friction Curve, $0.5\text{Li}_2\text{O}\cdot 0.5\text{Na}_2\text{O}\cdot \text{Al}_2\text{O}_3\cdot 2.0\text{SiO}_2$ Glass, Frequency 2024 HZ.

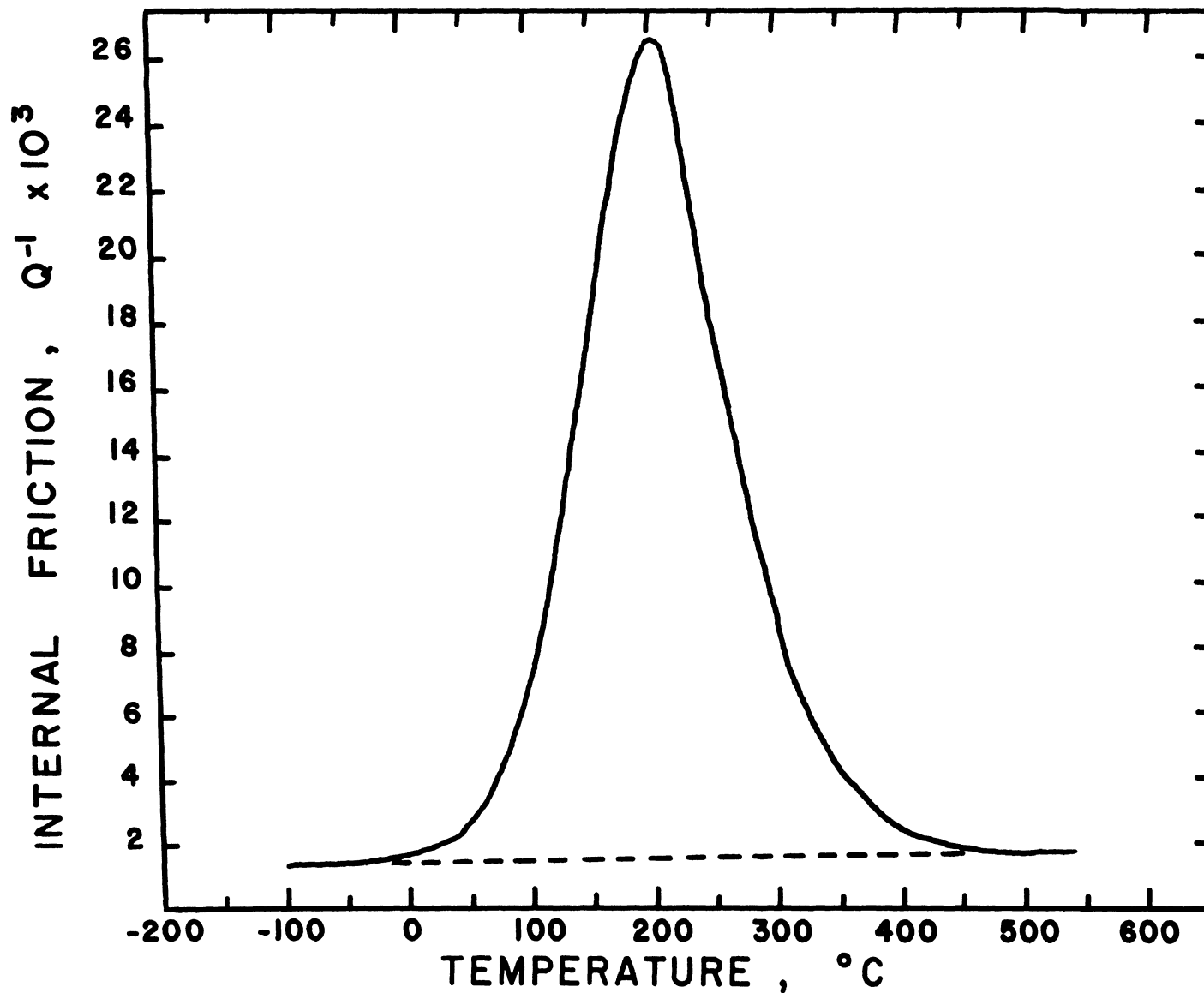


Figure 27. Internal Friction Curve, $0.5\text{Li}_2\text{O} \cdot 0.5\text{Na}_2\text{O} \cdot \text{Al}_2\text{O}_3 \cdot 2.0\text{SiO}_2$ Glass, Frequency 2751 HZ.

APPENDIX D

Derivation of Internal Friction Equation Based on Lognormal Distribution of Relaxation Times

Following is a derivation, beginning with the internal friction equation based on a single relaxation time, leading to the internal friction equation based on a lognormal distribution of relaxation times, equation (7) in the thesis.

For a single relaxation time

$$Q^{-1} = \Delta \frac{\omega \tau}{1 + \omega^2 \tau^2} \quad (15)$$

With a lognormal distribution of relaxation times

$$Q^{-1} = \int_{-\infty}^{\infty} K(\ln \tau) \Delta \frac{\omega \tau}{1 + \omega^2 \tau^2} d(\ln \tau) \quad (16)$$

where
$$\int_{-\infty}^{\infty} K(\ln \tau) d(\ln \tau) = 1 \quad (17)$$

$$K(\ln \tau) = \frac{1}{\beta \sqrt{\pi}} \exp \left\{ - \left[\ln(\tau / \tau_m) \right]^2 / \beta^2 \right\} \quad (18)$$

Let

$$Z = \ln(\tau / \tau_m) \quad (19)$$

$$\exp(Z) = \tau / \tau_m \text{ or } \tau = \tau_m \exp(Z) \quad (20)$$

$$K(Z) = \frac{1}{\beta \sqrt{\pi}} \exp \left\{ -Z^2 / \beta^2 \right\} \quad (21)$$

Now substitute (21) into (16) and change the limits appropriately

$$Q^{-1} = \int_{-\infty}^{\infty} \frac{1}{\beta \sqrt{\pi}} \exp \left\{ -Z^2 / \beta^2 \right\} \frac{\Delta \omega \tau}{1 + \omega^2 \tau^2} dZ \quad (22)$$

Put (20) into (22)

$$Q^{-1} = \int_{-\infty}^{\infty} \frac{\Delta}{\beta \sqrt{\pi}} \exp \left\{ -Z^2 / \beta^2 \right\} \frac{\omega \tau_m \exp(Z)}{1 + \omega^2 \tau_m^2 \exp(2Z)} dZ \quad (23)$$

APPENDIX D (continued)

Let $X = \ln \omega \tau_m$ (24)

$\exp(X) = \omega \tau_m$ (25)

So (23) becomes

$$Q^{-1} = \int_{-\infty}^{\infty} \frac{\Delta}{\beta \sqrt{\pi}} \exp \left\{ -z^2 / \beta^2 \right\} \frac{\exp(X+Z)}{1 + \exp [2(X+Z)]} dz \quad (26)$$

Let $U = z/\beta$ (27)

Use trigonometric identity

$$\frac{\exp(Y)}{1 + \exp(2Y)} = \frac{\operatorname{sech} Y}{2} \quad (28)$$

Substituting (28) and (27) into (26) yields

$$Q^{-1} = \frac{\Delta}{2 \sqrt{\pi}} \int_{-\infty}^{\infty} \exp(-U^2) \operatorname{sech}(X + \beta U) dU \quad (29)$$

This is also equation (7) in the thesis.

VII. BIBLIOGRAPHY

1. Lazan, B. J., "Damping Studies in Materials Science and Materials Engineering," Internal Friction, Damping, and Cyclic Plasticity, pp. 1-20, ASTM STP 378, 1964.
2. Kaelble, D. H., "Micromechanisms and Phenomenology of Damping in Polymers," Internal Friction, Damping, and Cyclic Plasticity, pp. 109-24, ASTM STP 378, 1964.
3. Demer, L. J., Bibliography of the Material Damping Field, WADC Technical Report 56-180 (PB-121437), June 1956.
4. Marlowe, M. O., and Wilder, D. R., Elasticity and Internal Friction Through the Kilocycle Range: Review and Annotated Bibliography, U.S.A.E.C. Research and Development Report IS-925, June 1964.
5. ASTM Symposium on Internal Friction, Damping, and Cyclic Plasticity Phenomena in Materials. Internal Friction, Damping, and Cyclic Plasticity, ASTM STP 378, 1964.
6. Conference on Internal Friction Due to Crystal Lattice Imperfections, Acta Met. 10 (4) 267-500 (1962).
7. Mason, W. P. (ed), Physical Acoustics, 5 vols. Academic Press, New York, 1963-68.
8. Forry, K. E., "Two Peaks in the Internal Friction as a Function of Temperature in Some Soda Silicate Glasses," Jour. Amer. Cer. Soc. 40 (2) 90-4 (1957).
9. Mohyuddin, I., and Douglas, R. W., "Some Observations of the Anelasticity of Glasses," P. Chem. Glass 1 (3) 71-86 (1960).
10. Day, D. E., and Rindone, G. E., "Internal Friction of Progressively Crystallized Glasses," Jour. Amer. Cer. Soc. 44 (9) 161-7 (1961).
11. Field, M. B., "Higher Temperature Internal Friction and Transport Mechanisms in Sodium Silicate Glasses," J. App. Phys. 39 (6) 2927-31 (1968).
12. Argon, A. S., "Delayed Elasticity in Inorganic Glasses," J. App. Phys. 39 (9) 4080-6 (1968).
13. Doremus, R. H., "Ionic Transport in Amorphous Oxides," J. Electrochem Soc.: Solid State Science 115 (2) 181-6 (1968).

VII. BIBLIOGRAPHY (continued)

14. Shelby, J. E., and Day, D. E., "Mechanical Relaxations in Mixed-Alkali Silicate Glasses: I, Results", Jour. Amer. Cer. Soc. 52 (4) 169-74 (1969). "II, Discussion", Jour. Amer. Cer. Soc. in press (1970).
15. Urnes, S., "Studies of the Sodium Distribution in Sodium Silicate Glasses by the Chemical Difference Method", P. Chem. Glass 10 (2) 69-71 (1969).
16. Taylor, S. W., "Internal Friction of Phase Separated Glasses", M.S. Thesis, University of Missouri-Rolla, (1969).
17. Day, D. E., and Rindone, G. E., "Properties of Soda Aluminosilicate Glasses: II, Internal Friction", Jour. Amer. Cer. Soc. 45 (10) 496-504 (1962).
18. Day, D. E., and Steinkamp, W. D., "Mechanical Damping Spectrum for Mixed-Alkali $R_2O \cdot Al_2O_3 \cdot 6SiO_2$ Glasses", Jour. Amer. Cer. Soc. 52 (11) 571-4 (1969).
19. Kirby, P. L., "The Mechanical Relaxation of Alkali Ions in a Borosilicate Glass", Jour. Soc. Glass Tech. 39 (9) 385-94 (1955).
20. Hopkins, I. L., and Kurkjian, C. R., "Relaxation Spectra and Relaxation Processes in Solid Polymers and Glasses", Physical Acoustics, Vol. II, Part B, Academic Press, New York 1965.
21. Fitzgerald, J. V., "Anelasticity of Glass: II, Internal Friction and Sodium Ion Diffusion in Tank Plate Glass, a Typical Soda-Lime-Silica Glass", Jour. Amer. Cer. Soc. 34 (11) 339-44 (1951).
22. Rotger, H., "Elastic After-Effects from Thermal Diffusion and Matter Diffusion by Periodic and Aperiodic Methods", Glastechn. Ber. 19 (6) 192-200 (1941).
23. Steinkamp, W. E., Shelby, J. E., and Day, D. E., "Internal Friction of Mixed-Alkali Silicate Glasses", Jour. Amer. Cer. Soc. 50 (5) 271 (1967).
24. Ryder, R. J., and Rindone, G. E., "Internal Friction of Simple Alkali Silicate Glasses Containing Alkaline-Earth Oxides: I, Experimental Results", Jour. Amer. Cer. Soc. 43 (12) 662-9 (1960). "II, Interpretation and Discussion", Jour. Amer. Cer. Soc. 44 (11) 532-40 (1961).

VII. BIBLIOGRAPHY (continued)

25. Graham, P. W. L., and Rindone, G. E., "Internal Friction Peak Caused by Condensation of Water on Barium Silicate Glasses", Jour. Amer. Cer. Soc. 50 (6) 336 (1967).
26. Copley, G. J., "Internal Friction Studies of the Dehydration of Sheet Glass", P. Chem. Glass 8 (1) 38-44 (1967).
27. de Waal, H., "Influence of Proton Exchange on Internal Friction in Alkali Silicate Glasses", Jour. Amer. Cer. Soc. 52 (3) 165-6 (1969).
28. Charles, R. J., "The Mixed Alkali Effect in Glasses", Jour. Amer. Cer. Soc. 48 (8) 432-4 (1965).
29. Copley, G. J., and Oakley, D. R., "Internal Friction Studies of the Stabilisation of Sheet Glass", P. Chem. Glass 9 (5) 141-7 (1968).
30. Nowick, A. S., and Berry, B. S., "The Zener Relaxation As a Distribution of Relaxation Times", Acta Met. 10 (4) 312-8 (1962).
31. Niblett, D. H., "Low-Frequency Measurements of the Bordoni Internal Friction Peak in Copper", J. App. Phys. 32 (5) 895-9 (1961).
32. Nowick, A. S., and Seraphim, D. P., "Magnitude of Zener Relaxation Effect - I, Survey of Alloy Systems", Acta Met. 9 (1) 40-8 (1961).
33. Li, C. Y., and Nowick, A. S., "Magnitude of Zener Relaxation Effect - II, Temperature Dependence of the Relaxation Strength in α AgZn", Acta Met. 9 (1) 49-58 (1961).
34. Forster, R., "New Method of Determination of Modulus of Elasticity and Damping", Z. Metallk. 29 (4) 109-15 (1937).
35. Miller, T. F., "Construction and Calibration of an Inverted Torsion Pendulum for Measuring the Internal Friction of Glass", M.S. Thesis, University of Missouri-Rolla, (1965).
36. Tomandl, G., and Oel, H. J., "Electrical and Mechanical After-Effects in Glass", Glastechn. Ber. 39 (10) 439-55 (1966).

VII. BIBLIOGRAPHY (continued)

37. Nowick, A. S., and Berry, B. S., "Lognormal Distribution Function for Describing Anelastic and Other Relaxation Processes, I. Theory and Numerical Computations", IBM J. Res. Dev. 5 297-311 (1961). "II. Data Analysis and Applications", IBM J. Res. Dev. 5 312-20 (1961).
38. Marx, J. W., and Sivertsen, J. M., "Temperature Dependence of the Elastic Moduli and Internal Friction of Silica and Glass", J. App. Phys. 24 (1) 81-7 (1953).
39. Taylor, H. E., Unpublished Thesis accepted for Ph.D., University of Sheffield, (1954).
40. Shelby, J. E., "Internal Friction of Mixed-Alkali Silicate Glasses", Ph.D. Thesis University of Missouri-Rolla, (1967).
41. McVay, G. L., "Diffusion and Internal Friction in Sodium-Rubidium Silicate Glasses", Ph.D. Thesis University of Missouri-Rolla, (1970).
42. Zener, C., Elasticity and Anelasticity of Metals, University of Chicago Press, Chicago, Illinois 1948.

VIII. VITA

David Wayne Moore was born on July 3, 1938, in St. Louis, Missouri. He received his primary education in Ferguson, Missouri, and graduated from the Hazelwood High School, St. Louis, Missouri, in June 1956. He received a B.S.M.E. Degree from Washington University in St. Louis in June 1960.

Immediately thereafter he was employed by McDonnell Douglas in St. Louis and attained the position of Senior Engineer-Strength before leaving in September 1966.

In September 1964 he enrolled at the Graduate Resident Center of UMR in St. Louis. In September 1966 he was employed as a graduate assistant in the Engineering Mechanics Department of the University of Missouri-Rolla. He received a M.S. in Engineering Mechanics from the University of Missouri-Rolla in June 1967. He then transferred to the Ceramic Engineering Department and in September 1967 he received a N.D.E.A. Title IV fellowship for his Ph.D. studies.

187437